VOT 78123

EXPERIMENTAL INVESTIGATION ON THE BEHAVIOUR OF THERMAL EFFLUENT IN FREE SURFACE FLOW

(KAJIAN EKSPERIMEN TERHADAP KELAKUNAN EFLUEN TERMA DI DALAM ALIRAN SALURAN TERBUKA)

ZULKIFLEE BIN IBRAHIM
DR. NOOR BAHARIM BIN HASHIM
ASSOC. PROF. ABD. AZIZ BIN ABDUL LATIFF
HERNI BINTI HALIM
NURUL HANA BINTI MOKHTAR KAMAL
NURYAZMEEN FARHAN BINTI HARON

RESEARCH VOTE NO:
78123

Jabatan Hidraul & Hidrologi
Fakulti Kejuruteraan Awam
Universiti Teknologi Malaysia

2008

ACKNOWLEDGEMENT

First and foremost, we would like to express our gratitude towards the Ministry of Higher Education (MOHE), Malaysia and Research Management Centre (RMC), Universiti Teknologi Malaysia (UTM) for their financial support for this research.

Our sincere appreciation to Dr. Suhaimi Abu Bakar (Department of Structure & Material, Faculty of Civil Engineering, UTM) for introducing the DPIV method and Dr. Yeak Su Hoe (Department of Mathematics, Faculty of Science, UTM) for the application of Maple software in this study.

We also would like to share our gratitude towards all staffs of Hydraulics and Hydrology Laboratory, Faculty of Civil Engineering, Universiti Teknologi Malaysia for their help and support during the experiments and work.

Last but not least, our greatest appreciation is extended to all the students who have involved in this study. This research will not be completed without their continuous hard work.

THE BEHAVIOUR OF SUBMERGED CROSS-FLOW THERMAL EFFLUENT DISCHARGE IN FREE SURFACE FLOW

(Keywords: Thermal effluent, multi-port diffuser, cross-flow, dispersion, near-field)

Thermal discharges such as from power station or industries polluting inland water bodies (rivers) causing degradation of water quality. The density of heated fluid is less than cold fluid and the positive buoyancy will force the heated fluid to disperse and spread at the ambient surface when it is discharged into the water bodies. Good understanding on thermal effluent behaviour in waterbodies leads good discharge management which can minimise the impact of thermal effluent pollution. An experimental study is conducted in the laboratory to investigate the mechanism of heat transport in free surface flow for ambient and thermal effluent flow rates. A multi-port diffuser pipe is placed at the channel bed in cross-flow direction to the ambient flow. Thermal effluent flow rates, Q_e used in the experiment are 0.05 liter/s and 0.133 liter/s. Meanwhile, two ambient flow rates, Q_a are fixed at 20 liter/s and 10 liter/s. The research focuses on thermal mixing process in near-field region. Among the parameters studied are effluent temperature, hydraulics characteristics of ambient flow (flow rate and velocity) and the characteristics of open channel including length, depth, and width. The dispersion profiles of thermal effluent are observed at various locations along the channel through the plotted isothermal lines. Meanwhile, the results of excess temperature ($\Delta T/T_e$) show that it decreases with the increasing of dispersion rate, K_T as the thermal effluent moves downstream of the channel. The changes of ambient temperature, ΔT are studied through the plotted graphs. The results show that mixing process occurs in near-field and far-field regions. The temperature differences in near-field region are higher than far-field region because the area experienced high thermal effluent temperature, T_e. Meanwhile, temperature differences in far-field region are low due to the effect of mixing between thermal effluent and ambient flow.

Key researchers :

Zulkiflee Ibrahim
Dr. Noor Baharim Hashim
Prof. Madya Abd. Aziz Abdul Latiff
Herni Halim
Nurul Hana Mokhtar Kamal
Nuryazmeen Farhan Haron

E-mail : zulkfe@utm.my
Tel. No. : 07-5531764
Vote No. : 78123

KAJIAN EKSPERIMEN TERHADAP KELAKUNAN EFLUEN TERMA DI DALAM ALIRAN TERBUKA

(Kata kunci: Efluen terma, paip peresap pelbagai liang, aliran menegak, medan dekat)

Pelepasan haba daripada stesyen janakuasa atau industri mencemarkan sungai dan menyebabkan pengurangan kualiti air. Ketumpatan air panas adalah rendah berbanding air sejuk dan daya keapungan positif akan menyebabkan air panas tersebar ke permukaan ambien apabila dilepaskan ke dalam sungai. Pemahaman yang baik dalam proses penyerakan effluen berhaba dalam sungai membawa kepada pengurusan pelepasan yang baik yang mana dapat mengurangkan kesan pencemaran haba. Kajian makmal dijalankan untuk mengkaji mekanisma pergerakan haba di dalam saluran terbuka pada kadar alir ambien dan effluen berhaba yang berbeza. Paip peresap pelbagai liang diletakkan di dasar saluran secara berserenjang dengan arah aliran ambien dalam sebuah saluran terbuka dengan kadar alir effluen berhaba, Q_e yang digunakan dalam eksperimen adalah tetap iaitu 0.05 liter/s dan 0.133 liter/s. Selain itu,dalam kajian ini, dua kadar alir ambien, Q_a yang ditetapkan iaitu 20.0 liter/s dan 10.0 liter/s digunakan. Proses percampuran effluen berhaba di dalam saluran tertumpu di kawasan medan dekat. Antara parameter yang terlibat dalam kajian adalah suhu effluen, ciri-ciri hidraulik aliran ambien (kadar alir dan halaju), dan ciri-ciri saluran terbuka termasuk panjang, dalam dan lebar. Corak serakan effluen berhaba pada setiap stesen cerapan di sepanjang saluran diperhatikan melalui plotan garisan isotermal. Sementara itu, *excess temperature*, $\Delta T/T_e$ menurun dengan peningkatan kadar serakan, K_T apabila semakin jauh pergerakan effluen terma di dalam saluran. Perubahan suhu ambien, ΔT dikaji melalui plotan graf. Keputusan yang diperolehi menunjukkan proses percampuran dalam kawasan medan dekat dan medan jauh. Perubahan suhu pada medan dekat adalah sangat tinggi kerana mengalami percampuran dengan effluen berhaba yang bersuhu tinggi, T_e. Manakala, perubahan suhu pada medan jauh adalah rendah kerana suhu effluen berhaba telah menurun akibat kesan proses percampuran dengan aliran ambien.

Penyelidik:

Zulkiflee Ibrahim
Dr. Noor Baharim Hashim
Prof. Madya Abd. Aziz Abdul Latiff
Herni Halim
Nurul Hana Mokhtar Kamal
Nuryazmeen Farhan Haron

E-mail : zulkfe@utm.my
No.Tel. : 07-5531764
No.Vot : 78123

TABLE OF CONTENTS

LIST OF TABLES

LIST OF FIGURES

LIST OF PHOTOS

LIST OF SYMBOLS

ν	=	kinematic viscosity
$\Delta\rho_c$	=	density difference between ambient and effluent flow
ρ_a	=	ambient density
g	=	gravity celerity
v	=	velocity of ambient flow
R	=	hydraulics radius of ambient flow
ΔT	=	temperature difference
T_e	=	effluent temperature
T_a	=	ambient temperature
Q_e	=	effluent flow rate
Q_a	=	ambient flow rate
K_T	=	dispersion rate
V	=	water volume in tank
A_d	=	area of of multi-port diffuser
R_e	=	Reynolds Number
F_D	=	Densimetric Froude Number
Fr	=	Froude Number
t_e	=	time taken to discharge thermal effluent
t	=	time taken to observe temperature in channel
t*	=	dimensionless time
u	=	ambient velocity
x	=	horizontal distance from discharge point
y	=	transverse distance from channel wall
z	=	vertical distance from bed of channel
d	=	diameter of port
H	=	flow depth

LIST OF APPENDICES

CHAPTER 1

INTRODUCTION

1.1 Introduction

In this new modern era, technologies keep developing each single day to fulfil human needs. With each new technology introduced, our natural environment will be more polluted as the volume from effluents created increases. Pollution can be defined as the existence or addition of some organics or inorganic substances into the environment that can damage part of the entire ecosystem. One of the most severe polluted media is the hydrosphere or usually known as water.

The water serves as one of the environmental continuum; along with soil and air which are dynamically interactive. In other words, with a change in one of these elements, it will generate the changes in the other elements. Despite dealt as a whole, these three elements always managed separately without considering the consequences for the other elements. The characteristic of water that flows and carries substances as it flows makes it one of the main pollutant transporters.

Hydrothermal pollution is one of water pollution forms. Hydrothermal pollution can be defined as a change of temperature in water bodies caused by human influences. Water used by power plants as coolant (i.e a fluid which flows through a device in order to prevent its overheating, transferring the heat produced by the device to other devices that utilize or dissipate it) is one of the main source of thermal pollution in rivers.

Excessive heat transferred into the water will typically decrease the concentration of dissolved oxygen in the water. This will result in the harming of aquatic life such as amphibians and copepods, increased in metabolic rate of aquatic life; resulting in the aquatic life consuming more food in shorter time compared to normal environment. As the environment changes, the population of aquatic life may decrease due to lack of food source, migration and in-migration of aquatic life to a more suitable environment. The food chain may be disrupted as competition for fewer resources took place.

From air temperature measurements constructed from land stations, a 0.5 °C warming occurred during the past 100 years in the United States (Schneider, 1989 in Singh and Hager, 1996). This might be the effects of human activities on the heat balance of the earth by direct release of stored energy at a rate faster than natural process, release of greenhouse gases and particulates and alteration of earth's albedo (Singh and Hager, 1996).

In preventing the rapid increasing of the earth temperature in the future, the effluents from the industrial and technologies need to be controlled. This will lessen the thermal pollution from occurring which will be affecting the stability of the ecosystem.

1.2 Statement of Problem

The number of power plants constructed lately has rise as the demand for power consumption has increased causing the higher volume of heated water discharged into rivers. With the increasing volume of discharged heated water, the ecosystem of the river may become unstable. Thermal pollution seems to affect the aquatic life immediately after the discharge. Evaporative water losses, dissolved oxygen production and consumption, primary biological productivity, toxicity of pollutants, fish growth and reproduction are examples of processes affected by water temperature changes. The most significant effect of temperature increase in rivers is the dissolved oxygen level. As the temperature increased, the level of dissolved oxygen decreased especially in the lower layers. In addition, because of the direct thermal shock, most aquatic life can be killed with the abrupt temperature change that goes beyond the tolerance limit of their metabolic systems.

Therefore, a study on the impact of thermal effluent released into a river system should be carried out. The behaviour of thermal effluent discharged in ambient flow is presented based on formula and calculation.

1.3 Objectives of the Research

This study describes an analysis of mixing of thermal effluent discharged from multiport diffuser to ambient flow. The objectives of the study are:

(i) to investigate the mechanism of heat transport in channel flow,

(ii) to establish the relationships among parameter including ambient flow conditions and heated flow properties, and

(iii) to investigate the impact of thermal discharges in inland water bodies.

1.4 Scope of Study

The scopes of this research comprise of two components: literature review and laboratory experiments. The rationale of literature review is to expand information and identify theories related to the study. Besides that, literature review is also carried out to judge against the existing theories and the studies that have been carried out earlier. According to literature review, several ideas and techniques to implement laboratory study are gained besides identifying parameters involved based on previous studies. The other important purpose of literature review is to identify the problems that may arise in data collection during the laboratory experiments.

Before conducting a research, other than giving the main idea of the research, literature review would help to determine the methods and techniques to be used in data collection. Parameters to be observed through the experiments also can be attained by reading literature review based on previous researches and theories. All of the information for the literature review are obtained from books, journals, encyclopedias, and from searched webs through the internet.

The laboratory experiment consists of the gathering of data by conducting series of experiments on the heat transport in open channel. Independent parameters such as effluent temperature and ambient discharge are adjusted to observe the relationship

between the parameters. In addition, Digital Particle Image Velocimetry (DPIV) method is used to investigate mixing processes related to a buoyant jet phenomenon.

CHAPTER 2

LITERATURE REVIEW

2.1 Introduction

The pollution of rivers which occurred due to the operation of the factories and power plants are getting worse if the discharges of the coolant from the plants into the rivers are not controlled. Obviously, the simplest method of disposing the heated waste water is to discharge them directly into the receiving water and allowed the natural forces to bring the water back to an equilibrium temperature. Thermal effluent discharge is released into the rivers using jet discharge system. The process of transporting effluent in open channel depends on the density of the effluent. Thermal effluent possesses lower density compared to ambient flow. Table 2.1 shows the thermal effluent sources which uses water as coolant based from the research done by Rensselaer Polytechnic Institute, New York. From Table 2.1, electric power generates the highest percentage of thermal effluent discharge with 81.2%.

Table 2.1: Thermal effluent sources with capacity and percentage (http://www.rpi.edu/dept)

Sources	Cooling Water (Billions of m^3)	Cooling Water (in %)
Electric Power	153.7	81.2
Primary Metals	12.8	6.76
Chemical and Allied Products	11.8	6.24
Others	10.9	5.80
Totals	189.2	100

An example of thermal effluent discharge through electric power plant is in Tanjung Bin Power plant. Tanjung Bin has been designated as the industrial centre for development of petrochemical and maritime industry under the Pontian District Plan 2002 to 2015 (Perunding Utama, 2003). This project of 2100 MW coal-fired power plant is priority in order to meet the country projected growth in electric demand. The project which has been identified by the Economic Planning Unit (EPU) of the Prime Minister's Department and Tenaga Nasional Berhad (TNB) has commercially operational by the end of August 2006.

Tanjung Bin power plant is located at the southwestern tip of Peninsular Malaysia along the western banks of the Sungai Pulai estuary. It also situated directly opposite to the existing Port of Tanjung Pelepas (PTP) and its southern frontage is the Straits of Johor as shown in Figure 2.1. The power plant with a nominal capacity of 2100 MW comprised of 3 turbine units of 700 MW capacity each. A once-through cooling water system is employed, with the intake located in the Sungai Pulai and the heated water discharged into the Straits of Johor to the southeast of the site.

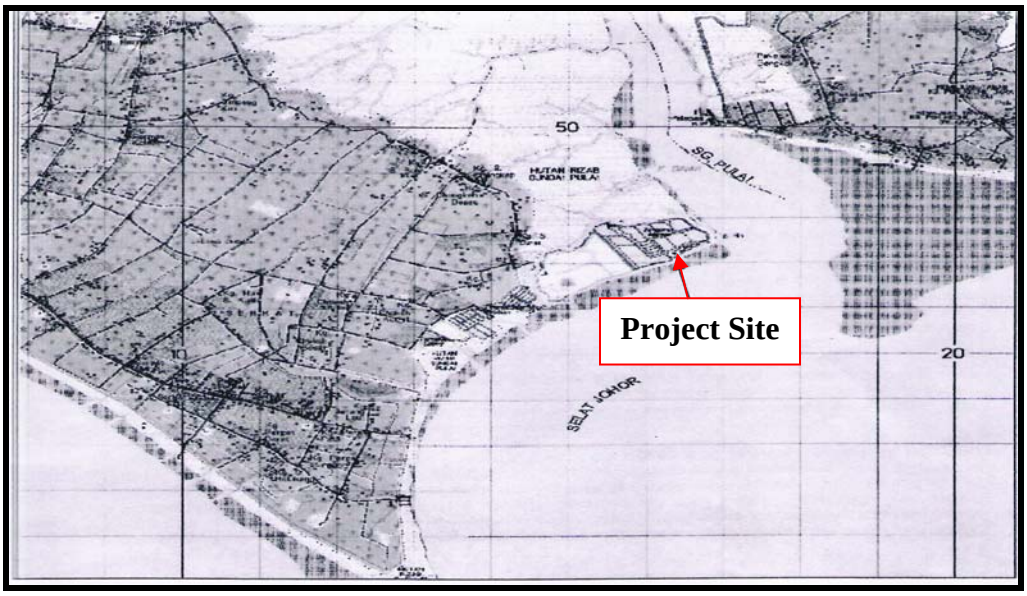

Figure 2.1: Location of Tanjung Bin Power Plant along the western banks of the Sungai Pulai (Perunding Utama Sdn. Bhd., 2003)

The power plant uses Sungai Pulai as the source of water for plant cooling processes. The water intake is located at the river mouth of Sungai Pulai. The warm water discharged from the plant will affect thermal regime of Sungai Pulai. The thermal pollution seems to only affect the communities immediately adjacent to the discharge. Thermal discharge is most noted in the tropical areas, where faunal organisms are near their maximum temperature tolerance.

In the worst-case scenario (during Mean Water Level after low water), a possibility of 8 ^{o}C in temperature rise when all the 3 turbine units are operating at full load. This will be only for a few hours in a day i.e during the morning and the evening peak period in electricity consumption. During other times, the expected load will be less than 90%, which resulted in a rise of less than 7 ^{o}C in condensers.

For the case of Tanjung Bin power plant, the site is surrounded by mangrove vegetation. Although mangrove vegetation is generally very tolerant to thermal pollution, the production rate has adversely affected producing fewer new seedlings (Perunding Utama, 2003). In case of Tanjung Bin power plant the heated water discharge produced an increase in water temperature to about 34 ^{o}C along the Sungai Pulai and to a distance of 400 m from the outfall. According to Perunding Utama (2003), temperature up to 40 ^{o}C does not visibly damage mangroves in short-term effects. Moreover both species composition and biomass of mangrove root communities are not affected adversely in temperature below 34 ^{o}C. However, the number of species dropped abruptly between 34 ^{o}C and 35 ^{o}C. Above this temperature the number inversely related to the water temperature.

For marine organisms, temperature of the water plays an important role in organic reproduction, growth, maturity and longevity. The effects of temperature are different for all organisms. An increase of 2.4 ^{o}C above the ambient level occurs during the commencement of the plant. However, the ecological impact from the thermal discharge is significantly only at the outfall itself with the temperature at the outfall between 40 ^{o}C to 41 ^{o}C. The high temperature plume is limited to the immediate area of the outfall (possibly not more than 50 m) and the temperature will fall rapidly with mixing of the water.

2.2 Terminologies

The definitions of some of the physical transport process and terminologies that would be significant in the research of heat transfer in open channel are:

i) Heat Transfer: A phenomenon of energy transfer which tended to establish thermal equilibrium. The energy would be moving from a region of higher temperature to the region with lower temperature. The energy in transit is termed heat.

ii) Thermal Pollution: A temperature change in natural water bodies caused by human influence with adverse environmental effects in aquatic system. A declination of the water bodies qualities in physical, chemical and biological aspects as the water bodies are polluted by the effluents of human activities such as the industrial effluents.

iii) Dispersion: A phenomenon of particles or cloud of contaminants scattering process by the combined effects of shear and transverse diffusion.

iv) Buoyancy: Can be defined as the gravitational body force that acted on a fluid of non-uniform density. Buoyancy produced as the effluent is of lighter density being discharged into the receiving water body of greater density. A temperature

variation can also resulted in the non-uniformity in fluid as the fluid with higher temperature had lighter density. So, it tended to float in the fluid with lower temperature with higher density. The buoyancy is created by burning or by heat conduction and radiation to the fluid. According to Singh and Hager (1996) the flux buoyancy force, F_o, due to the heat source is:

$$F_o = g\frac{\gamma H}{c_p} \quad , \tag{2.1}$$

where γ = the volume coefficient of thermal expansion (percentage of volumetric change per degree of temperature change)

H = the heat flux (energy per unit time)

C_p = specific heat at constant pressure (change in energy per unit mass of fluid and per degree of temperature change)

g = gravity acceleration

2.3 Characteristics of Thermal Effluent Discharge System

The hydrodynamic mixing process of any heated waste water discharge is governed by the interaction of ambient parameters in the receiving water body and by the thermal effluent parameters. Two main parameters for the mixing process that must be observed are the ambient conditions and the discharge conditions.

2.3.1 Ambient Parameters

Parameters in open channel represent hydraulics characteristic of ambient flow. According to Zimmerman and Geldner (1978) the parameters are open channel depth (y_0), open channel width (B_0), flow velocity (v_o), ambient water temperature (T_0), bed channel friction (k_s), formation of river bed, course of the main flow and flow direction. These parameters define type of flow in open channel either in laminar, transitional or turbulent condition.

2.3.2 Thermal Effluent Parameters

The parameters of thermal effluent discharge in ambient flow are jet diameter (d), flow velocity (u_e), effluent temperature (T_e), thermal effluent density (ρ_e), angle between effluent outwards direction and ambient flow (α).

All of the listed parameters are used in the calculation of the hydrodynamic mixing process. Different types of outlet may illustrate different types of mixing characteristics. For a single port discharge, the port diameter, the elevation above the bottom and its orientation provided the geometric features. Meanwhile for multi-port diffuser installations of the individual ports along the diffuser line, the orientation of the diffuser line, and construction details represented additional geometric features.

The buoyancy flux represented the effects of the relative density difference between the effluent discharge and ambient conditions in combination with the

gravitational acceleration. It is a measure of the tendency for the effluent flow to rise (positive buoyancy) or to fall (negative buoyancy) in the water column.

2.4 Heat Transport

Heat transport occurs during the existence of a temperature difference in a medium. Consequently, heat transport is defined as energy transfer due to temperature difference. The three basic modes of heat transport are conduction, convection and radiation (Stefan and Hondzo, 1996). Conduction arises by collision between molecules. Due to this process, conduction is sometimes called the "invisible" heat transport. Furthermore, convection is the heat transport in the presence of a moving fluid. Besides, radiation is heat transport that occurs by electromagnetic waves. All surface of finite temperature emit energy in the form of electromagnetic waves.

Water temperature levels and dynamics have a significant effect on aquatic ecosystems. Evaporative water losses, dissolved oxygen production and consumption, primary biological productivity, toxicity of pollutants, fish growth and reproduction are examples of processes affected by water temperature changes. For all of these causes, water temperature is considered as a key parameter of aquatic systems.

2.5 Mixing Processes

The mixing behaviour of thermal effluent discharge is governed by relationship between ambient conditions (geometric and dynamic characteristics) and discharge

characteristics (geometric and flux). For multi-port diffuser setting up, the orientations of the diffuser line and construction details are geometric features (Jirka *et. al*, 1996). The fluctuation characteristics are given by the effluent discharge flow rate, momentum fluctuation and buoyancy fluctuation.

A mixing process of an effluent continuously discharging into water body can be separated in two regions. In the near-field region, the initial jet characteristics of momentum flux, buoyancy flux, and outfall geometry influence the jet path and mixing. As the turbulent plume travels further away from the source, conditions existing in the ambient environment will control path. This region is known as far-field. Figure 2.2 illustrates near-field and far-field regions within effluent discharges in a river.

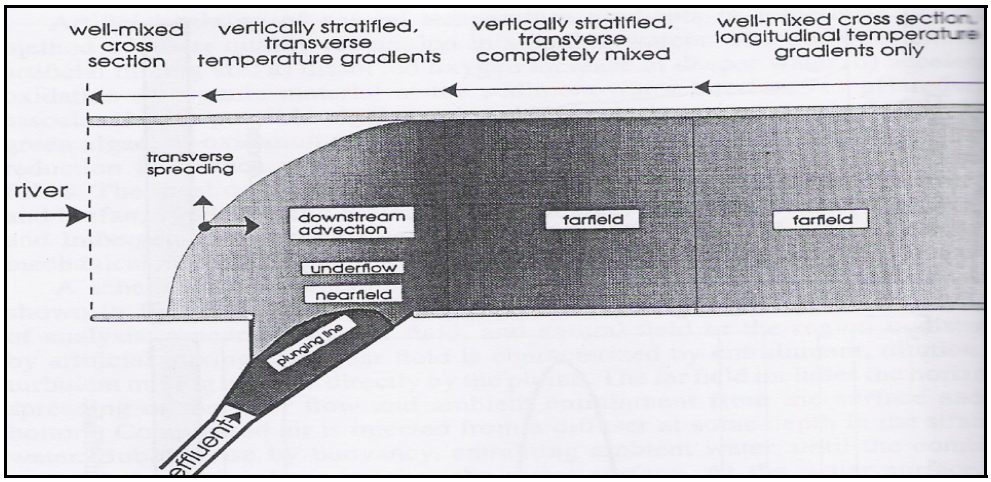

Figure 2.2: Near-field and far-field regions within effluent discharges in a river (Stefan and Hondzo, 1996)

2.5.1 Near-Field

Near–field is a region of the receiving water where the initial jet characteristics of momentum flux, buoyancy flux and outfall geometry influence the jet trajectory and mixing of the effluent discharge. Three types of near-field processes are submerged buoyant jet mixing, boundary relations and surface buoyant jet mixing.

For submerged buoyant jet mixing, the concept is that where both fluid momentum and pollutants are gradually diffused into the ambient field. The effluent flow from a submerged discharge port provides a velocity discontinuity between the discharged fluid and the ambient fluid. this condition produces shear force. The shearing flow breaks down rapidly into a turbulent movement. Any concentration of the discharge flow is diluted by ambient water through turbulent movement.

The near-field is usually highly three-dimensional and turbulent, with high dissipation of kinetic and potential energy of the discharged in the ambient fluid (Singh and Hager, 1996). The basic equations which describe the incompressible multi-dimensional fluid flow in the near-field written in index notation are the continuity, momentum and heat conservation equations. The equations are as follow:

Continuity equation:

$$\frac{\partial \overline{u_i}}{\partial x_i} = 0 \tag{2.2}$$

Momentum equation:

$$\frac{\partial \overline{u_i}}{\partial t} + \overline{u_j}\frac{\partial \overline{u_i}}{\partial x_j} = -\frac{1}{\rho_r}\frac{\partial \overline{p}}{\partial x_i} + \frac{\partial}{\partial x_j}\left(\nu \frac{\partial \overline{u_i}}{\partial x_j} - \overline{u'_i u'_j}\right) - g_i \beta (T - T_a) \tag{2.3}$$

Heat Conservation equation:

$$\frac{\partial \overline{T}}{\partial t} + \overline{u_i} \frac{\partial \overline{T}}{\partial x_i} = \frac{\partial}{\partial x_i}\left(K_m \frac{\partial \overline{T}}{\partial x_i} - \overline{u'_i T'} \right) \tag{2.4}$$

where u_i = instantaneous velocity component in the x_i direction (m/s)

K_m = molecular thermal diffusivity

T = instantaneous temperature (˚C)

x_i = wise stream direction (m)

Ambient currents and density stratification further affected the buoyant jet mixing. The buoyant jets are gradually deflected by the ambient currents into the current direction as shown in Figure 2.3 and thus induce additional mixing. The vertical acceleration within the buoyant jet is counteracted by the ambient density stratification eventually leading to trapping of flow at a certain level.

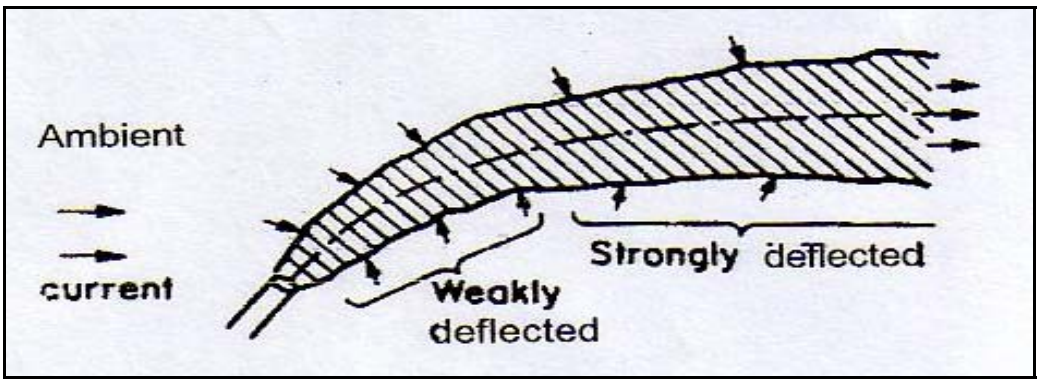

Figure 2.3: Ambient currents gradually deflect the buoyant jet into the current direction (Jirka, et al., 1996)

In case of multi-port diffuser, the individual round buoyant jets behave independently until they interact, or merge, with each other at a certain distance from the efflux ports. At a certain distance from the efflux ports, the individual round buoyant jets will merge, producing two dimensional buoyant jet planes as shown in Figure 2.4. Such plane buoyant jets resulting from a multi-port diffuser discharge in deep water can be further affected by ambient currents and density stratification.

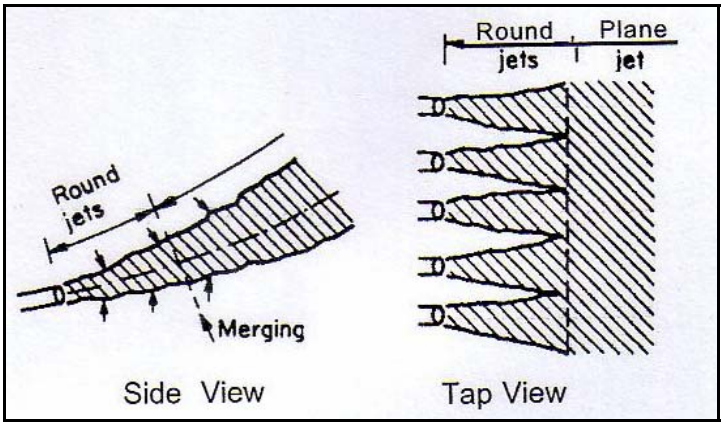

Figure 2.4: A two–dimensional buoyant jet plane

Another process of near field is boundary interaction processes. Ambient water bodies always have vertical boundaries. These include the water surface and the bottom, but in addition, internal boundaries may exist at pycnoclines. Pycnoclines are layers of rapid density change. Depending on the dynamic and geometric characteristics of the discharge flow, a variety of interaction phenomena can occur at such boundaries, particularly where flow trapping may occur.

2.5.2 Far-Field

Far-field is a region of the receiving water where the mixing processes are characterized by the longitudinal advection of the mixed effluent by the ambient current velocity. There are two processes at far–field. They are buoyant spreading processes and passive ambient diffusion processes.

Buoyant spreading processes are defined as the horizontally transverse spreading of the mixed effluent flow while it is being advected downstream by the ambient current. Such spreading processes arise due to the buoyant forces caused by the density difference of the mixed flow relative to the ambient density. They can be effective transport mechanisms that can quickly spread a mixed effluent laterally over large distances in the transverse direction, particularly in cases of strong ambient stratification.

In general, the passive diffusion flow grows in width and in thickness until it interacts. The strength of the ambient diffusion mechanism depends on a number of factors relating mainly to the geometry of the ambient shear flow and the amount of ambient stratification.

2.6 Cross-flow Mixing

The cross-flow mixing or also known as vertical diffusion by Singh and Hager (1996) in unstratified flow is usually estimated to be the same as the eddy viscosity; which is obtained from the logarithmic velocity distribution and the linear distribution of

shear stress from channel bed to water surface. According to Fisher et al. (1979) this method leads to:

$$e_z = \kappa_K u_* z (1- z/h) \quad (2.5)$$

where κ_K is von Karman coefficient, u_* is shear velocity, h is flow depth, and z is vertical coordinate measured upward from the bed.

Equation 2.5 gives a parabolic distribution of e_z and the "Reynolds analogy" which states it is used in the development of concentration distributions for suspended sediment which has been verified by Jobson and Sayre (1970) in Singh and Hager (1996) by means of an experimental research of the vertical mixing of dye in a flume. Averaging over the depth and $\kappa = 0.4$ gives:

$$\overline{e_z} = 0.067 d u_* \quad (2.6)$$

where d is depth of boundary layer.

The characteristics of spreading and entrainment change significantly as jets and plumes are deflected by a cross flow. Figure 2.5 shows vertical buoyant jet deflected by cross flow. The analysis for the effects of the cross flow is often carried out by considering the limitating cases of near-field and far-field separately. Wright (1977) in Singh and Hager (1996) has classified the flow into four limitating cases:

(i) mdnf (momentum-dominated near-field)
(ii) bdnf (buoyancy-dominated near-field)
(iii) mdff (momentum-dominated far-field)
(iv) bdff (buoyancy-dominated far-field)

From the experimental data obtained, the entrainment process in the near-field (mdnf and bdnf) is rather unaffected by the cross flow and is essentially the equivalent as the jets and plumes. While at the far-field process (mdff and bdff) are closely related to the vortex pair and is examined using a line impulse model. As in Figure 2.6, a vortex pair is formed as the jets bends over towards the direction of cross flow. Figure 2.7 shows ring vortices near the nozzles in close look.

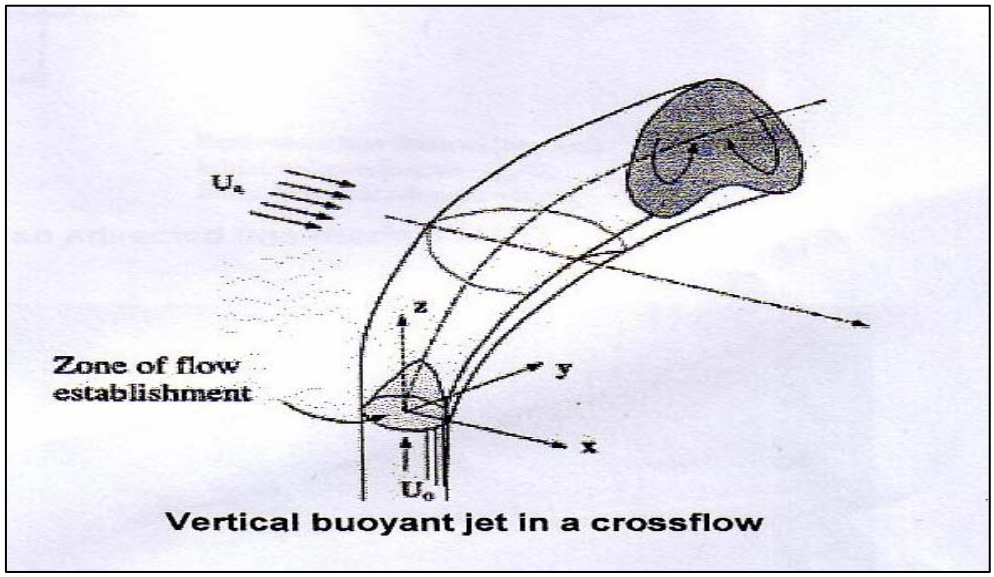

Figure 2.5: Vertical buoyant jet in cross-flow

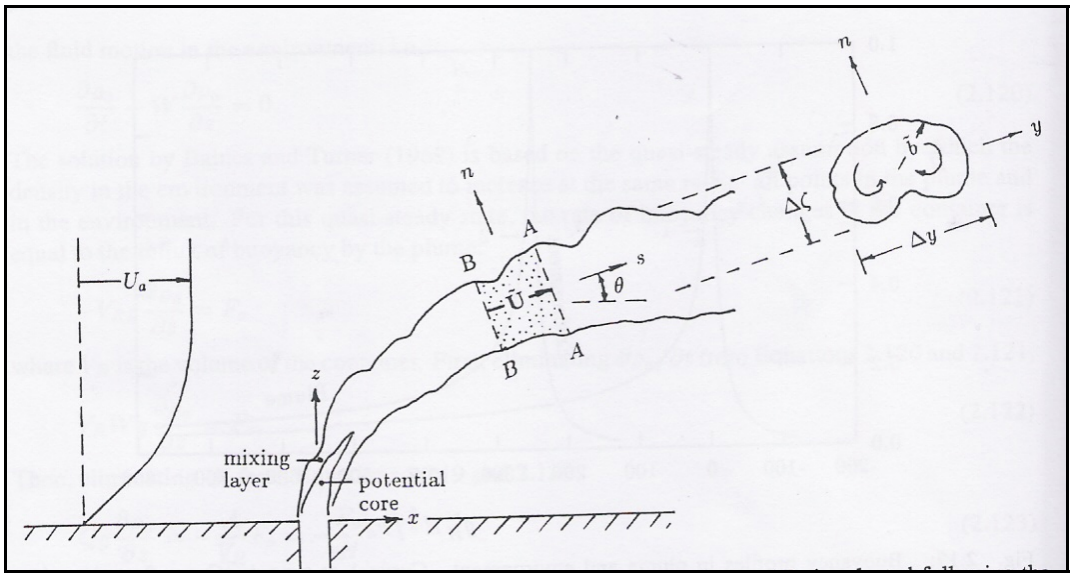

Figure 2.6: A vortex pair in cross-flow

Figure 2.7: Ring vortices near the nozzles

2.7 Co-flow Mixing

Co-flow mixing is the condition where effluent is flow parallel water body flow. Figure 2.8 shows co-flow mixing of effluent in water bodies. Also known as transverse dispersion, co-flow takes place in rivers due to two categories of mechanism, namely turbulence and intertwining of time-averaged streamlines, with turbulent mixing between the streamlines.

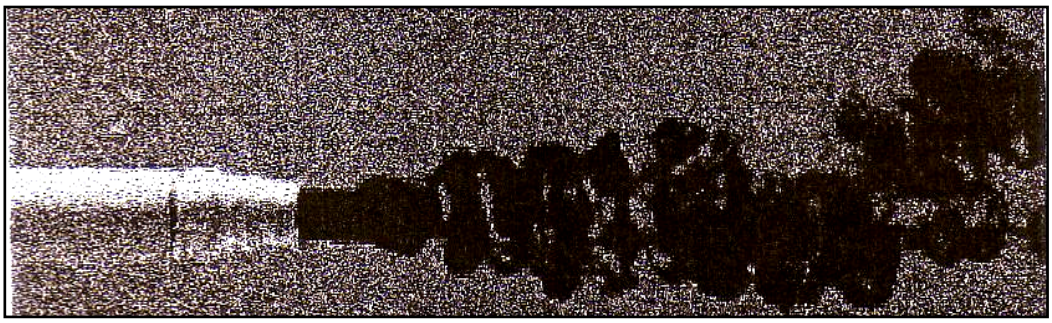

Figure 2.8: Co-flow mixing of effluent in water body

The conditions that may create turbulence in rivers are bed shear and separation at bed irregularities, flow circulation in pools of pool-and-riffle streams. Other than that, flow separation at the inside of sharp bends or at the ends of groins, jetties, or other bank protection also causes turbulence in rivers. In addition, flow confinement structures and apparently by transverse shear associated with the transverse distribution of longitudinal velocity also cause turbulence in rivers.

Streamlines intertwine occurs because of continual splitting and convergence of streamlines in braided rivers, flow around bed irregularities in rivers with irregular cross sections and secondary flow (e.g. helical flow in bends). Tracer test is conducted as it is

the most reliable method to obtain transverse dispersion coefficients (k_y) for a river. In conditions that a tracer test is not applicable, there are some general but very limited results which can be used as guidance for the expected value of k_y. Generalized values for k_y are normally given as non dimensional values for α_y which is defined as k_y / Hu_* with H as average depth.

Previous researchers observed that, cross-flow mixing is better than co-flow mixing. According to Afidah Murni et.al. (2004) and Ruzanna (2005), cross-flow discharge produces higher dispersion rate compared to co-flow discharge**.**

2.8 Jet Mixing

In many researches of jet mixing, several factors are taken into consideration in identifying jet process in mixing. Jet and plumes are defined as turbulent shear flows driven by sources of momentum and buoyancy respectively. The mixing and dispersion of the contaminants with the environment depend on the momentum and buoyancy flux of the discharge, along with the velocity distribution and density stratification of the receiving environment. Jet mixing is related directly to the inertia of the turbulent eddies. The buoyant force in the plume produces the inertia which leads to mixing.

Meanwhile, in co–flow jet mixing, inertia force manipulate the mixing process compared to buoyancy. Furthermore, immediate momentum is manipulated by buoyancy and influence the formation of mixing zone in the flow.

The Froude number is the ratio of mean velocity to the celerity of the gravity waves.

$$Fr = \frac{V}{\sqrt{gL}} \tag{2.7}$$

where, V = mean velocity (m/s)
g = acceleration of gravity (m/s^2)
L = characteristic length (or can be hydraulic depth, H in open channel) (m)

with Fr < 1 (subcritical flow)
Fr = 1 (critical flow)
Fr > 1 (supercritical flow)

In cross-flow discharge, buoyancy force reduces effluent dispersion rate in vertical direction. Buoyancy effects is stated by Densimetric Froude number as shown in equation 2.8 (Martin and McCutcheon, 1999):

$$F_D = \frac{u_c}{\sqrt{gH\frac{\Delta\rho_0}{\rho_a}}} \tag{2.8}$$

where , $\Delta\rho_o$ = difference of effluent density and ambient density
ρ_a = ambient density, kg/m^3
u_c = turbulent velocity at water surface parallel to the jet, m/s
H = vertical depth of jet, m
g = gravitational acceleration, m/s^2

Densimetric Froude number, F_D represents type of flow in jet mixing. F_D equals to 1 ($F_D = 1$) shows that the flow in jet mixing is critical while F_D less than 1 ($F_D < 1$)

indicates that the flow is subcritical flow. F_D more than 1 ($F_D > 1$) denote that the type of flow in jet mixing is supercritical flow (Martin and McCutcheon, 1999).

The Reynolds number represents the effect of viscosity relative to inertia which is given as:

$$\mathrm{Re} = \frac{uL}{\nu} \tag{2.9}$$

where, u = flow velocity, m/s

L = Characteristic length (also can be considered as hydraulic radius, R for open channel), m

υ = kinematic viscosity, m^2/s

Turbulent flow has Re greater than 12,500 while Reynolds number for transitional flow is between 500 and 12,500. Laminar flow has Re less than 500 (Chow, 1959).

2.9 Excess Temperature and Dispersion Rate

Excess temperature, $\Delta T/T_{e,}$ is a normalisation of the temperature difference, ΔT, in the water flow after the thermal effluent is being discharged. The equation for $\Delta T/T_e$ is :

$$\Delta T/T_e = \frac{T_x - T_a}{T_e} \tag{2.10}$$

where T_a is ambient temperature (^{0}C), T_e is effluent temperature (^{0}C), T_x is observed temperature (^{0}C) at distance x along the channel (Kuang and Lee, 2001).

Effluent dispersion rate, K_T , can be defined as the cooling and dilution rate of the thermal effluent discharged in the water flow. It is important in determining the efficiency of a pipe diffuser system. Dispersion rate always inversely proportion to the excess temperature. A small changes of temperatures gives higher dispersion rates. Ambient flow velocity and distance from multiport diffuser influence dispersion rate in open channel. from K_T can be calculated using equation 2.11 (Pinheiro et al., 1997):

$$K_T = \frac{T_e - T_a}{T_x - T_a} \tag{2.11}$$

where T_a is ambient temperature (^{0}C), T_e is effluent temperature (^{0}C), T_x is observed temperature at distance x along the channel (^{0}C).

2.10 Digital Particle Image Velocimetry (DPIV) Method

In recent years, the measuring techniques of Digital Particle Image Velocimetry (DPIV) are broadly used to investigate mixing processes related to buoyant jets phenomenon (Law and Wang, 1991). DPIV requires the projection of a laser sheet onto the flow field at successive time intervals and the subsequent capturing of the images detailing the position of seeding particles that reflect the laser light. Analysis of the difference in positions of the particles reveals the Langragian velocity distribution of the flow field.

The present setup improves on the accuracy of the measurements by adopting fully digital approaches. The DPIV setup can measure at sub-pixel accuracy (typically 0.1 pixels). Through cross- correlation of two successive images in MATLAB software using correlation of URAPIV file, the velocity vectors are readily determined with DPIV. Figure 2.9 shows example of velocity vectors of buoyant jet using DPIV method.

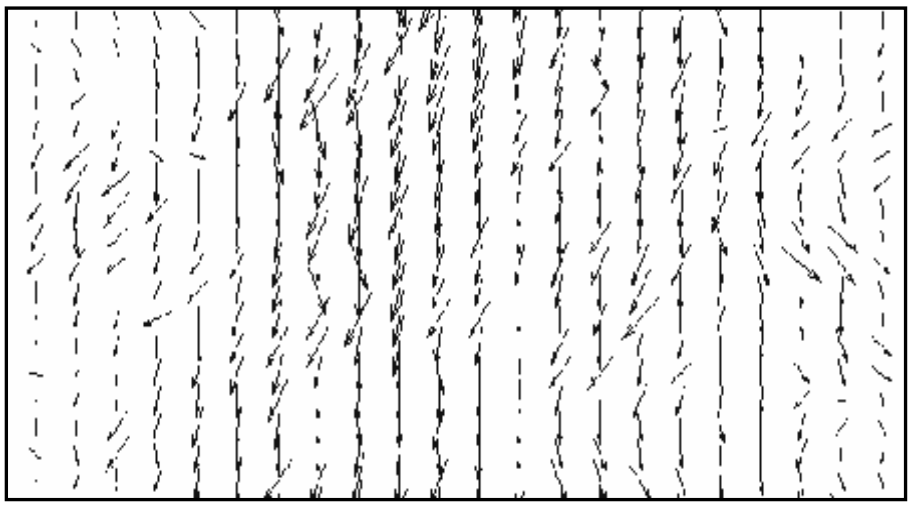

Figure 2.9 : Example of velocity vectors of buoyant jet using DPIV method.

2.11 Previous Researches

Previous researc**hes** on thermal effluent discharge in open channel flow have been carried out by several researches all over the world. Kim and Il (1999), Zimmermann and Geldner (1978), Davidson et al., (2001), Davies et al., (1994) are some of the researchers that actively involved in thermal effluent discharge studies.

2.11.1 Study by Kim Dae Geun and Il Won Seo (1999)

Kim Dae Geun and Il Won Seo have carried out an experimental study on mixing of thermal effluent discharged from multi–port diffuser using three–dimensional grid–based numerical model. For this study, the internal boundary is treated as a line patch. Discharge flowrate, $Q_{N,}$ from a cell of numerical slot diffuser can be determined using equation 2.12.

$$Q_N = n.Iq.b.L.u(x) \tag{2.12}$$

where n is number of ports included in a cell of numerical slot diffuser, Iq is shape constants, b is effective width of single jet, L is port spacing and u(x) is jet centerline velocity.

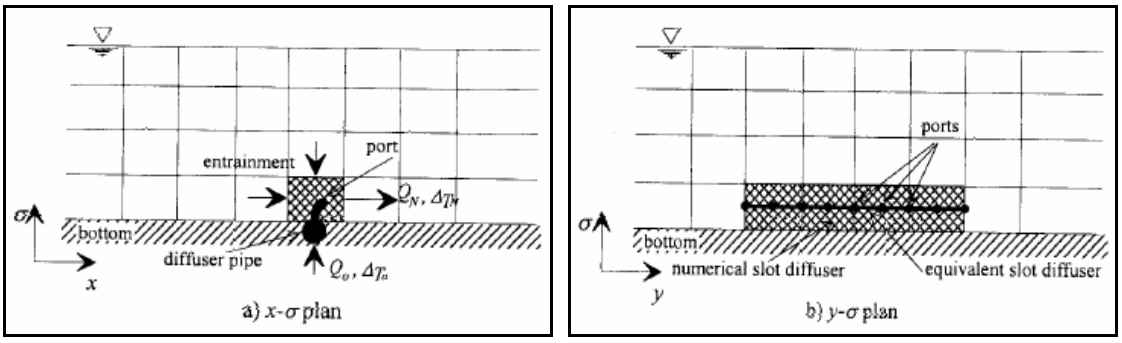

Figure 2.10: Internal boundary condition for submerge multiport diffuser.

Discharge excess temperature, ΔT_N from a cell of numerical slot diffuser can be determined by using equation 2.13.

$$\Delta T_N = \frac{Q_N}{Q_o} \Delta T_o \quad (2.13)$$

where Q_o is discharge flow rate from ports in a cell of numerical slot diffuser, ΔT_o is discharge excess temperature from multi-port diffuser.

The research is concluded that pattern of thermal plume simulated by the numerical model are agreeable with the observed thermal plume. Furthermore, excess temperature is decreasing as ambient water depth is increasing. The result confirms the previous study in which dilution of Tee shape diffuser varies sensitively with ambient water depth. The simulation by the numerical model is accordance with experimental results.

2.11.2 Study by Zimmermann and Geldner (1978)

Zimmermann and Geldner are German researches who have applied thermal modelling to understand about the effects of thermal pollution on Rhine River. The experiments are carried out to determine the influence of the ambient flow rate upon the isothermal pattern of the river. From the results, it shows that the ambient flow rate and the usage of different depth influenced the isothermal patterns. Based on the experiments, the equations for the temperature rise as the effect from the thermal effluent discharged into the river was then obtained.

The specific heat, W_x, for a cross-section part of a river at a distance, x, with the flow rate, Q, at the upstream of river is:

$$W_x = \Delta T_x . \rho_w . C_w . Q \qquad (2.14)$$

The thermal capacity transport of the river, W_A, is obtained from the actual discharge rate and the temperature difference, ΔT as:

$$W_A = \Delta T_x . \rho_w . C_w . Q \qquad (2.15)$$

where ρ_w is density of water and C_w is the specific heat of water.

The temperature of thermal effluent in the river will decrease gradually to downstream due to the thermal dissipation into the atmosphere through the water surface. The dissipation process could be explained in exponential law as:

$$\frac{\Delta T_x}{\Delta T_0} = \exp \frac{(-k.x)}{\rho_w . C_w . V_0} \qquad (2.16)$$

where V_0 is the mean velocity and k is the water dissipation coefficient.

2.11.3 Study by Davidson et.al. (2001)

Davidson, Gaskin and Wood have carried out a study on symmetry jet in co-flow to produce a general equation for turbulent flow. The predictions of the theory are verified for the no cross-flow case and the cases where the jet or plume is ejected vertically or horizontally into a very small cross-flow.

The results of experiments in which a buoyant jet is released in the same direction as the horizontal ambient flow, show that outside the turbulent region the entrainment velocities can be represented with uniform flow and the appropriate sink. Direct measurement of the strength of the sink allows the transition from weakly to strongly-advected behaviour to be determined.

The study utilised optical measurement technique of Laser Induced Fluorescence (LIF) and Particle Image Velocimetry (PIV) system. LIF technique is used to measure thermal effluent dispersion patterns when the effluent is discharged into ambient flow. Meanwhile, PIV system is used to acquire molecul displacement in the flow.

Average jet buoyancy velocity, $\bar{u}$ for a study without cross-flow is as stated in equation 2.17:

$$\bar{u} = Ue^{-(\frac{r}{b})^2} \tag{2.17}$$

where $\bar{u}$ = average jet buoyancy velocity

U = velocity at centre line

r = radius for average of jet buoyancy velocity, $\bar{u}$

b = radius when $\bar{u}/U$ equals to $1/e$

e = buoyancy time at centre line

Meanwhile, the equation to obtain average flow rate for a small cross-flow is as follow:

$$\frac{d\bar{q}}{ds} = 2\pi b\alpha U_e \tag{2.18}$$

where U_e is effluent velocity.

2.11.4 Study by Davies et.al. (1994)

Davies et.al. have been conducted a laboratory experiments on the behaviour of vertical round buoyant jets in shallow homogeneous cross-flows. Shallow depth effects are found to be significant in increasing dilution. This is through their effect on the constant of proportionality in the power law relationship between the normalized dilution and x/z, where z is the vertical coordinate of the dilution minimum at a distance x downstream of the source.

The densimetric Froude number, F_o of the jet for this experiment is given as:

$$F_o = \frac{u_j}{\sqrt{g' D}} \tag{2.19}$$

where u_j = mean velocity through a circular orifice

g' = modified gravitational acceleration at the source, $g(\rho_c - \rho_H)/\rho_c$

D = diameter of the orifice

ρ_c = density of cool water

ρ_H = density of heated water

The magnitudes of excess temperatures recorded at any centre-line location could be used to compute minimum dilution values, S_m , defined here as

$$S_m(x) = \frac{T_H - T_C}{T_{\max}(x) - T_C} \tag{2.20}$$

Where T_H = hot water temperature

T_C = cold freshwater temperature

$T_{max}(x)$ = maximum temperature for different values of downstream distance x from the source

CHAPTER 3

RESEARCH METHODOLOGY

3.1 Introduction

Research methodology is divided into two elements; literature review and experimental setup. According to literature review, several ideas and techniques to implement laboratory study are gained besides identifying parameters involved based on previous studies. The other important purpose of literature review is to identify the problems that may arise in data collection during the laboratory experiments. The experiment that carried out will study the dispersion pattern of thermal effluent in the flume in near-field and far-field region. Other than that, excess temperature and dispersion rate along the flume in three different depths also studied in the experiment.

3.2 Experimental Setup

An experimental study is carried out at the Hydraulics and Hydrology laboratory in Faculty of Civil Engineering, Universiti Teknologi Malaysia. The laboratory study is conducted to investigate mechanism of heat transport in open channel flow. Rhodamine B dye is mixed with heated water as a tracer. The experiment is carried out using a glass flume with 7.0 m long, 0.3 m wide and 0.3 m deep as shown in Photo 3.1. Other instruments used are including YSI 30 Salinity, Conductivity, and Temperature (SCT) (Photo 3.2), multi-port diffuser with each hole is 12 mm in diameter (Photo 3.3), a submersible pump, a PVC pipe and thermal effluent tank as shown in Photo 3.4. Meanwhile, Figure 3.1 shows the setup of experimental work.

Photo 3.1: 7.0 m long, 0.3 m wide and 0.3 m deep glass flume

Photo 3.2: YSI 30 Salinity, Conductivity, and Temperature (SCT)

Photo 3.3: PVC pipe with 5 holes and 12 mm diameter each multi-port diffuser.

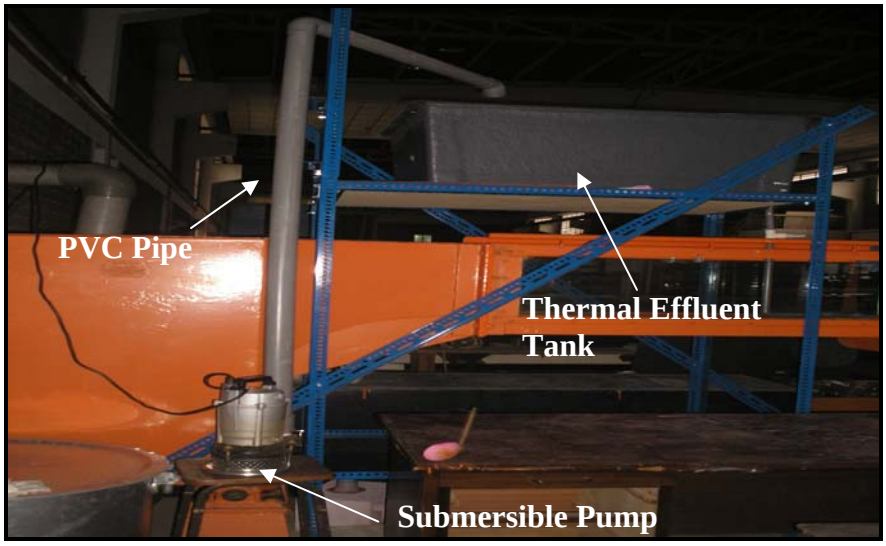

Photo 3.4: A submersible portable pump, a PVC pipe and overhead thermal effluent tank

Figure 3.1: The setup of experimental work

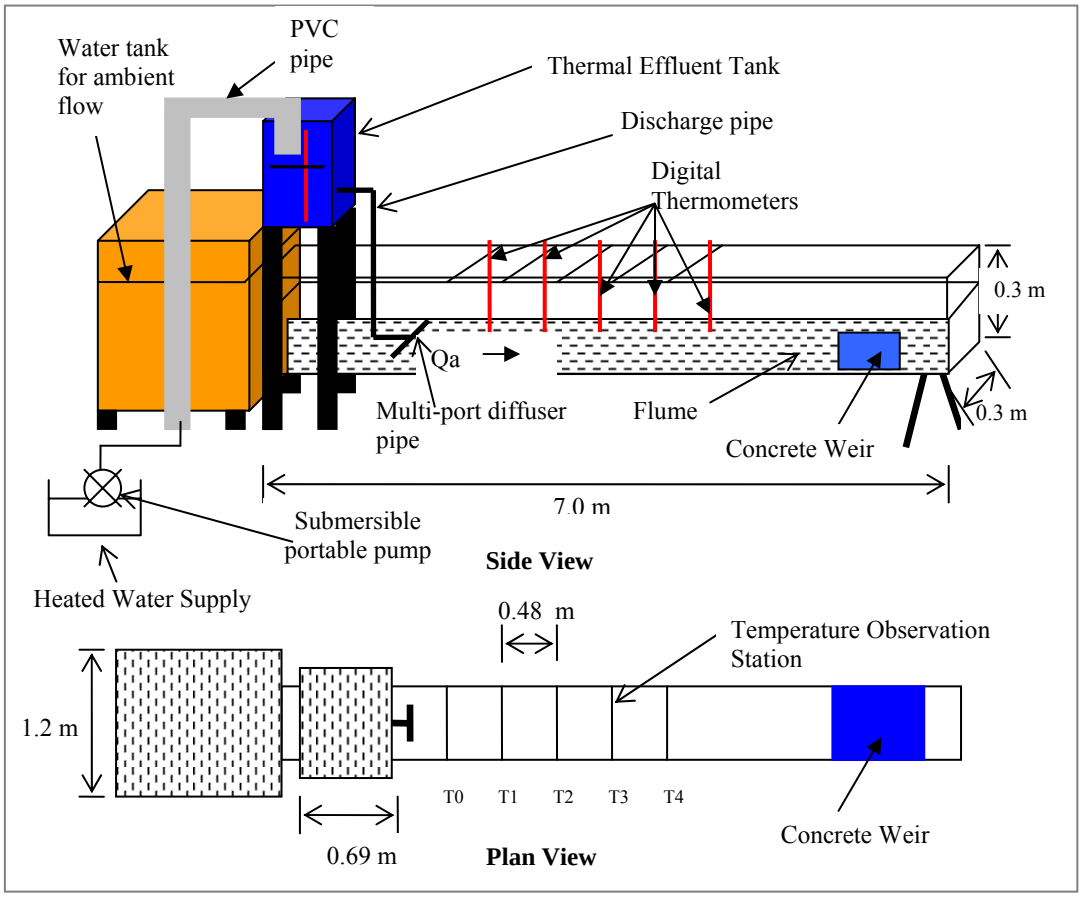

Figure 3.1 shows the setup for experimental work of thermal effluent discharge in open channel flow. The flume has glasses wall. A weir is placed near the end of flume to elevate the level of ambient flow. Hot water from heated water supply is pumped into an overhead tank. At the initial of the experiment, heated water is discharged in flume for 210 seconds. The plan view shows 5 stations of data collection and each station is 480 mm apart. Digital thermometers and YSI SCT are placed in the middle and side of flume at each station to observe temperature during experimental work.

3.3 Dimensional Analysis

Dimensional analysis is a mathematical technique using dimensions where variables are combined into dimensionless products and eliminating insignificant variables. Dimensional analysis gives qualitative rather than quantitative relationships, but when combined with experimental procedures it may be made to supply quantitative results and accurate predictions equations (Zulkiflee I., 2006).

List of parameters related to thermal effluent discharge in open channel flow are as follows:

i. ambient flow rate, Q_a [L^3T^{-1}]
ii. effluent flow rate, Q_e [L^3T^{-1}]
iii. temperature difference, $\Delta T = T_x - T_a$ (^{0}C)
iv. effluent temperature, T_e (^{0}C)
v. vertical distance from channel bed, z [L]
vi. transverse distance from channel wall, y [L]
vii. longitudinal distance from multi-port diffuser, x [L]

viii.	cross-sectional area of the channel, A	$[L^2]$
ix.	width of the channel, B	[L]
x.	diameter of port, d	[L]
xi.	density difference, $\Delta\rho = \rho_a - \rho_e$	$[ML^{-3}]$
xii.	gravity celerity, g	$[LT^{-2}]$
xiii.	viscocity, υ_a	$[L^2T^{-1}]$
xiv.	hydraulics radius, R	[L]
xv.	viscosity, υ_e	$[L^2T^{-1}]$
xvi.	ambient density, ρ_a	$[ML^{-3}]$
xvii.	ambient velocity, U_a	$[LT^{-1}]$
xviii.	effluent velocity, U_e	$[LT^{-1}]$

Using dimensional analysis, the relationship between $\frac{\Delta T}{T_e}$ with other non-dimensional groups can be written as:

$$\frac{\Delta T}{T_e} = \Phi\left[\frac{x}{d}, \frac{y}{d}, \frac{z}{d}, \frac{Q_a}{Q_e}, \frac{u_a R}{\upsilon_a}, \frac{u_e d}{\upsilon_e}, \frac{Ua}{\left(\frac{\Delta\rho}{\rho a} gH\right)^{\frac{1}{2}}}\right]$$

The fifth and sixth terms in equation 3.1 are Reynolds numbers for ambient and thermal effluent flows, respectively. Meanwhile, the last term can be defined as densimetric Froude number, F_D which is calculated and discussed in section 4.

3.4 Measurement of Ambient Flow Rate

Measurement of ambient flow rate is carried out by using rating curve which is developed earlier and as shown in Figure 3.2. Before the experimental work is carried out, the velocities of the ambient flow at different depths of water is determined. Using continuity equation as stated in equation 3.1 the flow rates are calculated:

$$Q = Au_a \tag{3.1}$$

where Q is discharge of ambient, m^3/s, u_a is velocity of ambient flow, m/s, and A is cross-sectional area of water filled in the flume, m^2.

A rating curve presents the relationship between flow rate and flow depth in the flume.

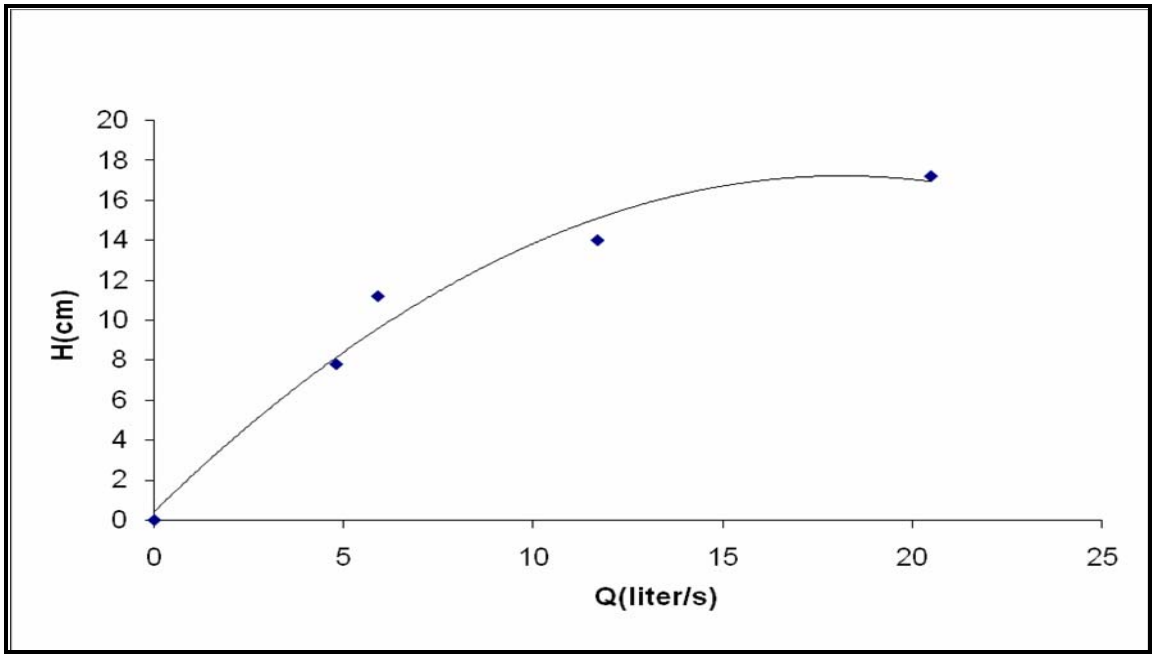

Figure 3.2: The developed rating curve for the study

3.5 Measurement of Ambient Velocity

The measurement of ambient velocity is carried out by using 2-axis valeport electromagnetic current meter model 802. Velocity of ambient flow is measured by locating the current meter sensor in different flow depths (0.2H, 0.4H and 0.8H where H is the total depth of ambient). Automatically, the velocity reading will be shown on the display unit. Photo 3.5 shows the current meter used in the study.

Photo 3.5: 2 axis electromagnetic Valeport current meter model 802

3.6 Measurement of Thermal Effluent Flow Rate

Thermal effluent flow rate depends on the diameter of discharge ports. Equation 3.3 is used to calculate thermal effluent flow rate. Meanwhile equation 3.4 is used to calculate jet velocity of thermal effluent discharged from the diffuser.

$$Q_e = \frac{V}{t} \tag{3.3}$$

where Q_e is effluent discharge (m^3/s), V is specified volume of water in overhead tank, (m^3), t is time taken to empty specified volume of water in the tank (s).

From equation 3.3, the thermal effluent discharge is divided into 5 as the total of effluent thermal diffuser is 5.

$$U_{jet} = \frac{Q_{effluent}}{5A_p} \tag{3.4}$$

where U_{jet} is jet velocity for each port (m/s), Q_e is effluent discharge (m^3/s), A_p is cross-sectional area of each port (m^2).

3.7 Measurement of Water Temperature

Water temperature in the flume is measured using YSI SCT and digital thermometers. Temperature observation is carried out at 5 stations along the flume. Readings of water temperature in channel flow are taken at every 15 seconds. Photo 3.6 shows the location of digital thermometer in flume.

Photo 3.6: Locations of digital thermometer at different depths in the flume

Tables 3.1 to 3.4 show observation stations for water temperature along x, y and z- axes.

Table 3.1: Temperature observation stations along x-axis

Station, Tx	Horizontal distance from multi-port diffuser, x (mm)	x/d
Tx_0	0	0
Tx_1	360	30
Tx_2	840	70
Tx_3	1320	110
Tx_4	1800	150

(Note: d is diameter of multi-port diffuser which is equal to 12 mm)

Table 3.2: Temperature observation stations along y-axis

Station, Ty	Transverse distance from channel wall, y (mm)	y/d
Ty_1	75	6.25
Ty_2	150	12.5

(Note: d is diameter of multi-port diffuser which is equal to 12 mm)

Table 3.3: Temperature observation stations along z-axis for Q_a of 10 liter/s

Station, Tz	Vertical distance from channel bed, z (mm)	z/H
Tz_0	22.9	0.2
Tz_1	53.6	0.4
Tz_2	99.5	0.8

(Note: H is depth of water which is equal to 110 mm)

Table 3.4: Temperature observation stations along z- axis for Q_a of 20 liter/s

Station, Tz	Vertical distance from channel bed, z (mm)	z/H
Tz_0	30	0.2
Tz_1	70	0.4
Tz_2	130	0.8

(Note: H is depth of water which is equal to 170 mm)

3.8 Experimental Procedures

There are several procedures that need to be followed in carrying out the experiment. The experimental procedures are:

(i) Determine ambient flow rate from developed rating curve.
(ii) Pumped heated water into thermal effluent overhead tank and set its temperature at 45 °C.
(iii) Open effluent valve to allow heated water discharge into ambient flow.
(iv) Record the time as thermal effluent is discharged from the overhead tank.
(v) Record temperature readings at each station every 15 seconds.
(vi) Repeat steps 1 to 5 for the next experiment.

3.9 Data Analysis

Data collected from experiment are further analysed. The analysis is focused on effluent dispersion patterns, excess temperature and dispersion rate. Surfer 32 software is used to plot isothermal lines on effluent dispersion patterns. The excess temperature and dispersion rate are presented in form of plotted graphs. Equations of excess temperature and dispersion rate are produced via Maple 9.5 software.

3.9.1 Effluent Dispersion Patterns

Densimetric Froude number, F_D and Reynolds number, Re are parameters used in the analysis to classify the condition of ambient flow. Meanwhile, isothermal lines are used to visualise dispersion pattern in near-field and far-field regions. The dispersion is greatly influenced by turbulent flow. Furthermore, it is expected that the principle of positive buoyancy is applicable in this study.

3.9.2 Excess Temperature and Dispersion Rate

The excess temperature, $\frac{\Delta T}{T_e}$ (Kuang and Lee, 2001) and dispersion rate, K_T (Pinheiro et. al., 1997) can be calculated from equations 2.10 and 2.11, respectively.

$$\frac{\Delta T}{T_e} = \frac{T_x - T_a}{T_e} \tag{2.10}$$

$$K_T = \frac{T_e - T_a}{T_x - T_a} = \frac{T_e - T_a}{\Delta T} \tag{2.11}$$

where T_a is ambient water temperature (^{0}C), T_e is effluent water temperature (^{0}C), and T_x is observed water temperature (^{0}C) at distance x along the channel.

CHAPTER 4

FINDINGS AND DISCUSSION

4.1 Introduction

In this chapter, discussions of experimental findings are focused on :

(i) thermal effluent dispersion patterns in ambient flow,

(ii) spatial excess temperature ($\Delta T/T_e$),

(iii) dispersion rate (K_T) in open channel flow and

(iv) temporal ambient temperature difference (ΔT) with dimensionless time (t*)

Water temperature readings are observed at five stations along the channel. As mentioned earlier in Chapter 3, they are $x_0/d = 0$, $x_1/d = 30$, $x_2/d = 70$, $x_3/d = 110$ and $x_4/d = 150$. Temperature observation at every station is carried out at three normalised depths of $z/H = 0.2$, $z/H = 0.4$ and $z/H = 0.8$ at the side of channel ($y/d = 2.1$) and center of the channel ($y/d = 12.5$). The definitions of the notations are as follows:

x = horizontal distance from discharge point (mm)
y = transverse distance from channel wall (mm)
z = vertical distance from channel bed (mm)
d = diameter of port equal to 12 mm
H = total flow depth (mm)
z/H = 0.2 => lower layer of flow
z/H = 0.4 => middle layer of flow
z/H = 0.8 => upper layer of flow

4.2 Ambient Flow Characteristics

In the initial stage of the experiment, a rating curve is produced to relate the depth of the ambient flow for different flow rates. From the rating curve, for flow rate of 20.0 liter/s the corresponding ambient flow depth is 17 cm and for 10.0 liter/s the corresponding depth is 13 cm. Meanwhile, two thermal effluent flow rates of 0.05 liter/s and 0.133 liter/s are used in the experiment study. Table 4.1 shows the ratio of ambient and thermal effluent flow rates used in the study.

Table 4.1: Ratio of effluent and ambient flow rates (Q_e/Q_a) used in the study.

Q_e (liter/s) / Q_a (liter/s)	0.133	0.05
	Q_a/Q_e	
20	150.38	400
10	75.19	200

The Reynolds number, Re represents the effect of viscosity force relative to inertial force. Meanwhile, the gravity effect on the flow is represented by a ratio of inertial force to gravity force known as the Froude number, Fr. Thus, Re determines either the flow laminar, transitional or turbulent while Fr determines either the flow is subcritical, critical or supercritical.

Densimetric Froude number, F_D, represents the ratio of inertia to buoyancy forces. However for this research, the application of densimetric Froude number is not suitable. As density difference, $\Delta\rho$, between the ambient flow and the effluent is small, the calculated F_D number has classified the mixing flow in the flume as supercritical. Thus, the Froude number is used to classify the flow condition.

Table 4.2: Calculated Fr and Re of the ambient flow in the experimental study.

Q_a (liter/s)	$Fr = \frac{u}{\sqrt{gH}}$	$\mathrm{Re} = \frac{uR}{\nu}$
20	0.303	37,105
10	0.227	21,161

Table 4.2 shows the calculated Froude and Reynolds numbers of ambient flow in the study. The Fr value for both ambient flow rate is smaller than 1. Thus the ambient flow is classified as subcritical flow. The velocity of ambient affects the dispersion rate of the thermal flow. The ambient flow is classified as turbulent since the Re value is greater than 12,500.

4.3 Velocity Profile

It is important to identify the velocity of the ambient at a certain depth of ambient flow in order to obtain the velocity profile of the flume. The ambient flow usually influences the dispersion rate of heated effluent in the channel. The size of the channel, the channel roughness, the channel bed slope, and velocity of ambient low govern the velocity and discharge.

The velocity of the ambient is measured using a 2-axis electromagnetic current meter. The 2-axis electromagnetic current meter measures the average velocity of the ambient flow in the x and y axes of the flow. The velocity of the ambient flow readings are taken at the maximum possible points for data collection. In this case, for a flow depth of 160 mm, 13 sets of readings are taken for every 10 mm vertically from the depths of 20 mm to 140 mm depth.

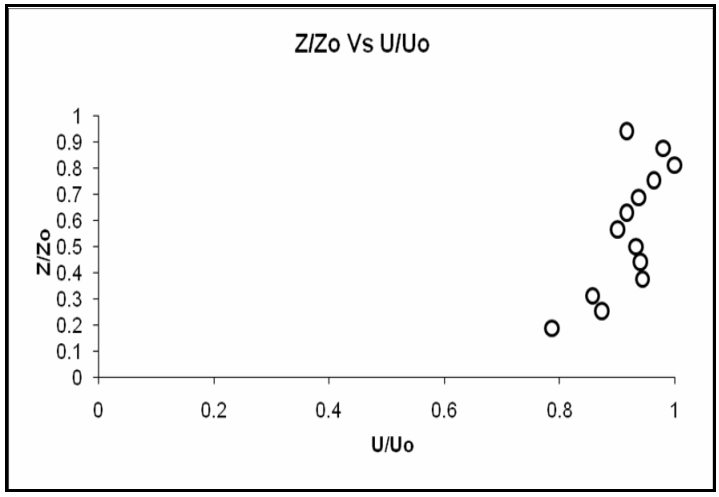

Figure 4.1: Normalised ambient velocity

The velocity of the ambient will differ based on the ambient flow discharge. The data obtained need to be normalized. U_0 is the maximum velocity, while the Z_0 is the maximum depth of flow. From the graph plotted (Figure 4.1), it can be concluded that

at the middle of the ambient flow, the velocity is higher than at the bed and the surface of the flow. The friction at the bed and walls surfaces of the channel reduces the velocity.

Photo 4.1: Trajectory of thermal effluent discharge in the channel (Q_e= 0.05 liter/s, Q_a=10 liter/s)

Photo 4.2: Trajectory of thermal effluent discharge in the channel (Q_e=0.133 liter/s, Q_a=10 liter/s)

Based from Photo 4.1 and 4.2, it can be seen that for different volume of thermal effluent discharged, the trajectory is different. For larger volume of thermal effluent, the thermal effluent is trajected higher right after discharged into the ambient flow for the same ambient flow velocity. Thus, the temperature is higher at the surface right after the multi-port diffuser for the higher volume of thermal effluent.

Meanwhile for the smaller volume of the thermal effluent, the trajectoty of the thermal effluent is lower. Thus, the surface temperature is lower right after the discharge as the thermal effluent is being drifted by the ambient flow furher downstream before reaching surface.

4.4 Digital Particle Image Velocimetry (DPIV) Method

The velocity vectors of the ambient flow can be determined by using Digital Particle Image Velocimetry (DPIV) method. DPIV requires the projection of a laser sheet onto the flow field at successive time intervals and the subsequent capturing of the images detailing the position of seeding particles that reflect the laser light. Through cross- correlation of two successive images in MATLAB software using correlation of URAPIV file, the velocity vectors of the flume can be determined.

Figure 4.2a and Figure 4.2b show the velocity vectors for ambient flow rates of 20 liter/s and 10 liter/s, respectively. In the experiment, it is clearly seen that the water particles move randomly in the flume. This indicates that the ambient flow is in turbulent condition. This finding supports the calculated Reynolds number as described in section 4.2, where ambient flow is turbulent condition.

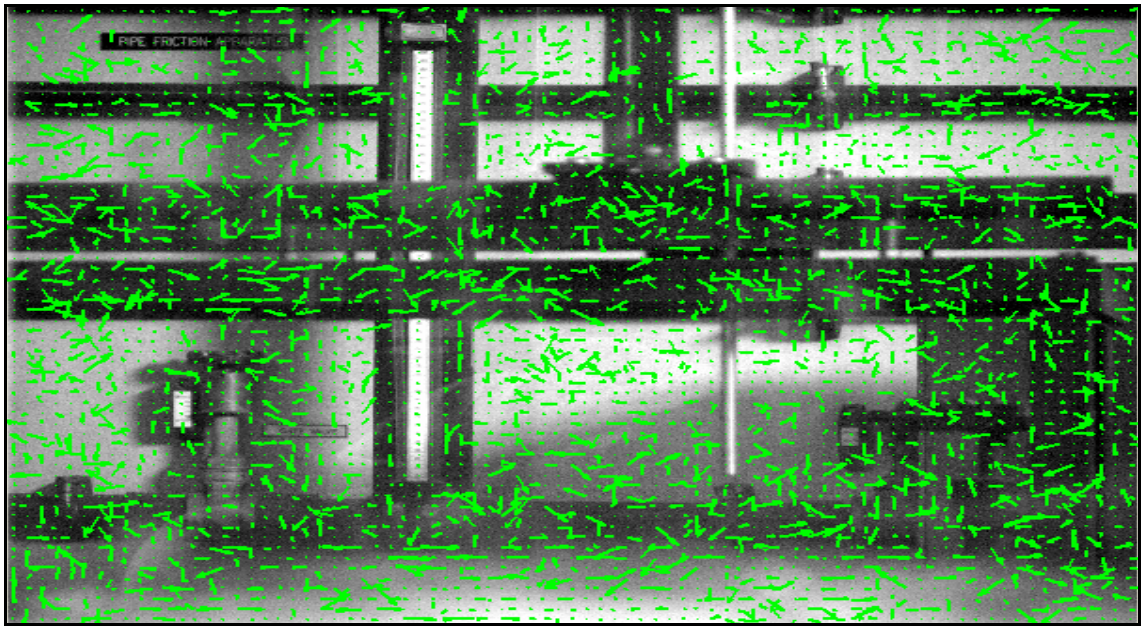

Figure 4.2a: Velocity vectors using DPIV method for ambient flow of Q_a of 20 liter/s

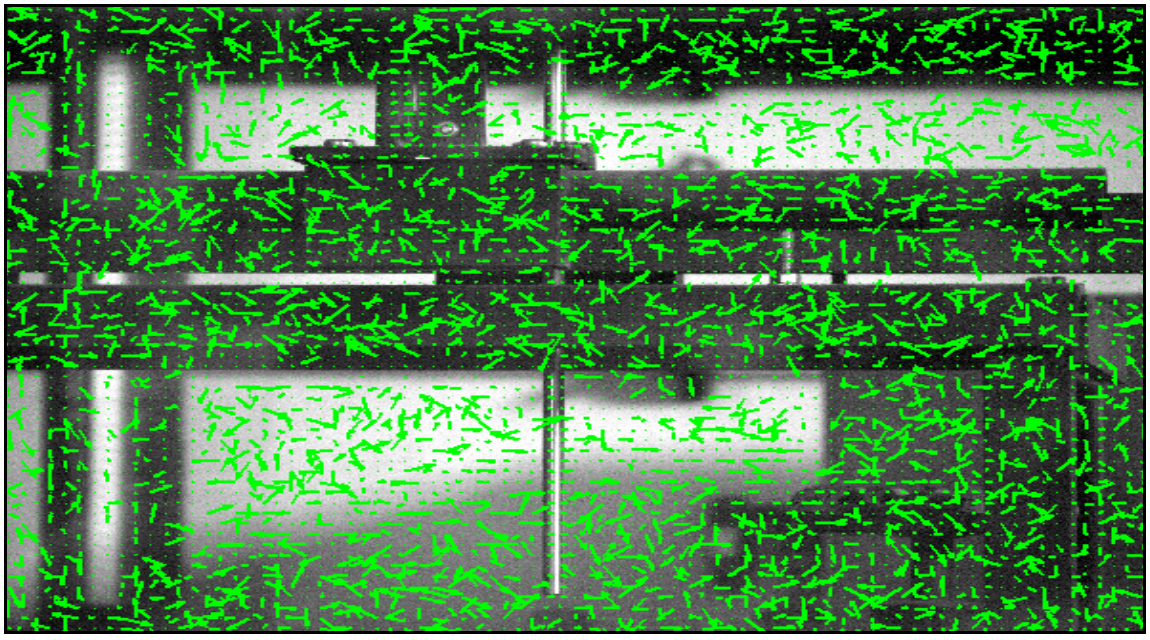

Figure 4.2b: Velocity vectors using DPIV method for ambient flow of Q_a of 10 liter/s.

4.5 Effluent Dispersion Patterns

The cross-sectional effluent dispersion patterns for the cross-flow discharges are illustrated from temperature difference (ΔT) at every station. Temperature difference in the mixed water is caused by density stratification between the ambient flow and the effluent discharged. In the experiment, there are five stations measuring mixed water temperature difference in the channel. The stations are located at $x_0/d = 0$, $x_1/d = 30$, $x_2/d = 70$, $x_3/d = 110$ dan $x_4/d = 150$. Based on calculated ΔT, isotherm lines are plotted to observe effluent dispersion patterns along the channel.

The discussion of the dispersion pattern is divided into two zones; the near-field and far-field region. For the near-field region, the discussion is at station x/d=30. Meanwhile station x/d=110 is used for far-field region discussion. The dispersion pattern figures are developed using software Surfer 32.

4.5.1 Dispersion Pattern in Near-Field (x/d=30)

Station x/d = 30 is selected to study the behaviour effluent dispersion in the near-field region. Figures 4.3a shows cross-sectional temperature difference using isotherm lines at x/d = 30 for Q_e of 0.05 liter/s. Meanwhile, Figure 4.3b shows cross-sectional effluent dispersion patterns at x/d = 30 for higher Q_e of 0.133 liter/s. The ambient flow rate for both figures is 20 liter/s. In Figure 4.3a, heated water moves to the surface of the channel and disperse uniformly. Figure 4.3b also displays similar phenomenon where the heated water moves to the surface of the channel but not well-dispersed.

The movement of the thermal effluent to the top of the channel is known as positive buoyancy, where fluid with less density (i.e. heated water) moves upward (Fischer et. al, 1979). This phenomenon results water temperature at surface is higher than the temperature at the bottom of the channel. Both of the figures show that thermal effluent starts to disperse in the channel when reaches x/d = 30.

In the Figure 4.3a, the highest temperature difference is 0.7 ^{0}C, while the lowest is 0 ^{0}C. Meanwhile in Figure 4.3b, the highest temperature difference is at the bottom of the channel with 0.28 °C and the lowest temperature difference is at the top side of the channel with temperature difference of 0 °C. Higher temperature difference at the bottom of the channel for Q_e of 0.133 liter/s is due to the higher volume of thermal effluent discharged into the channel as compared to for the case of Q_e of 0.05 liter/s.

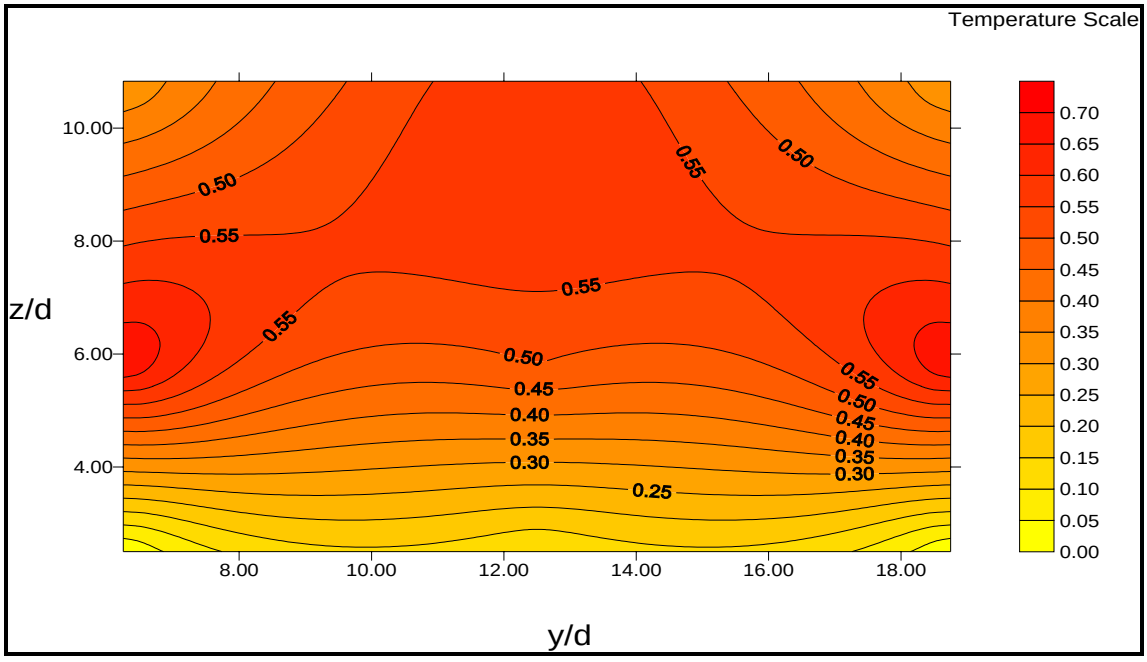

Figure 4.3a : Cross-sectional ΔT (in ^{0}C) at x/d = 30 for Q_a = 20.0 liter/s and Q_e = 0.05 liter/s

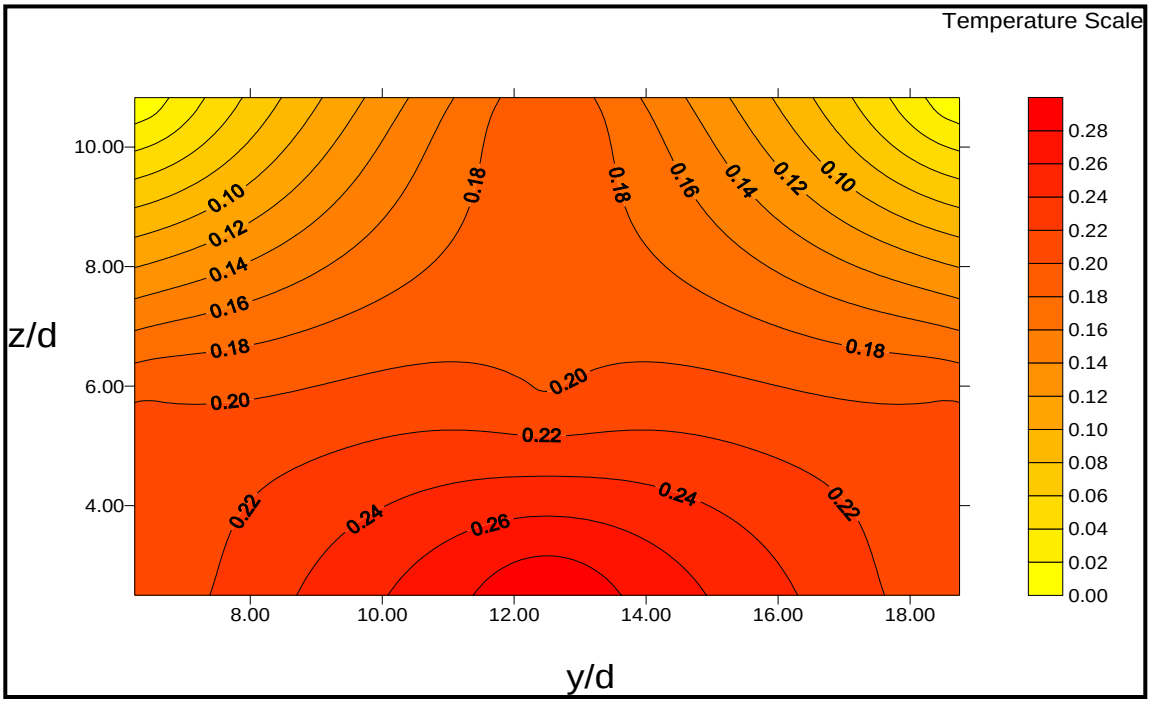

Figure 4.3b : Cross-sectional ΔT (in ^{0}C) at x/d = 30 for Q_a = 20.0 liter/s and Q_e = 0.133 liter/s

Meanwhile, Figures 4.4a and 4.4b show effluent dispersion temperature difference for ambient flow rate of 10 liter/s using isotherm lines at x/d at 30 for Q_e of 0.05 liter/s and 0.133 liter/s, respectively. Figure 4.4a shows that the heated water moves to the middle layer of the channel while in Figure 4.4b the heated water remains at the bottom of the channel.

The movement of the thermal effluent to mid-flow depth of the channel in Figure 4.4a shows that positive buoyancy has influenced the dispersion pattern, where fluid with less density (i.e. heated water) moves upwards to the water surface. However, because of the smaller effluent flow rate, the dispersion rate decreases. In other words, the dispersion rate is directly proportional to mass flow rate.

Both of the figures show that thermal effluent start to disperse in the channel at x/d = 30. In Figure 4.4a, the highest temperature difference is 0.65 ^{0}C while the lowest is 0.15 ^{0}C. Based on Figure 4.4b, the highest temperature difference is 0.48^{0}C while the lowest is 0.08 ^{0}C. The thermal effluent is still at the bottom of the channel in Figure 4.4b as the volume of thermal effluent is bigger. Longer distance is needed to dilute the thermal effluent.

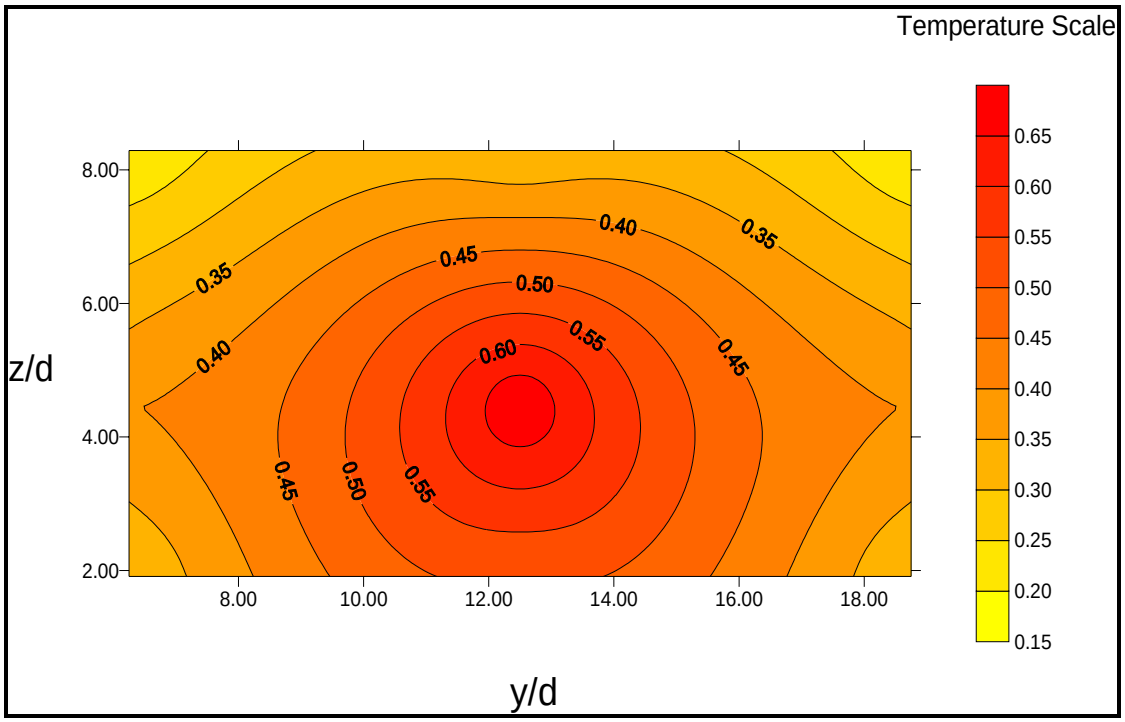

Figure 4.4a : Cross-sectional ΔT (in ^{0}C) at x/d = 30 for Q_a = 10.0 liter/s and Q_e = 0.05 liter/s

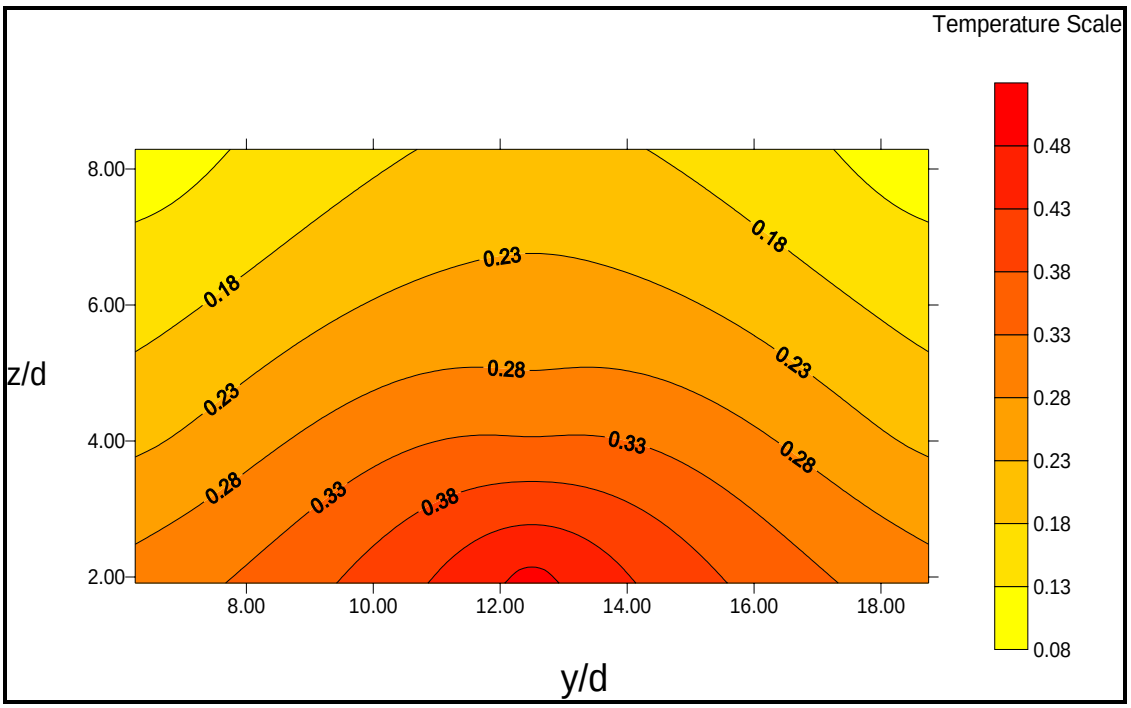

Figure 4.4b : Cross-sectional ΔT (in ^{0}C) at x/d = 30 for Q_a = 10.0 liter/s and Q_e = 0.133 liter/s

4.5.2 Dispersion Pattern in Far-Field (x/d = 110)

Figures 4.5a shows isothermal lines to visualise the thermal effluent dispersion for Q_a of 20 liter/s at far-field region for Q_e of 0.05 liter/s Meanwhile, Figure 4.5b shows cross-sectional effluent dispersion patterns at x/d of 110 for Q_e of 0.133 liter/s. The highest temperature difference in Figure 4.5a is located at the top of the channel which is 0.5 ^{0}C while the lowest temperature difference is 0 ^{0}C at bottom of the channel. From observation, the result shows that minimum thermal stratification occurs in the far-field region.

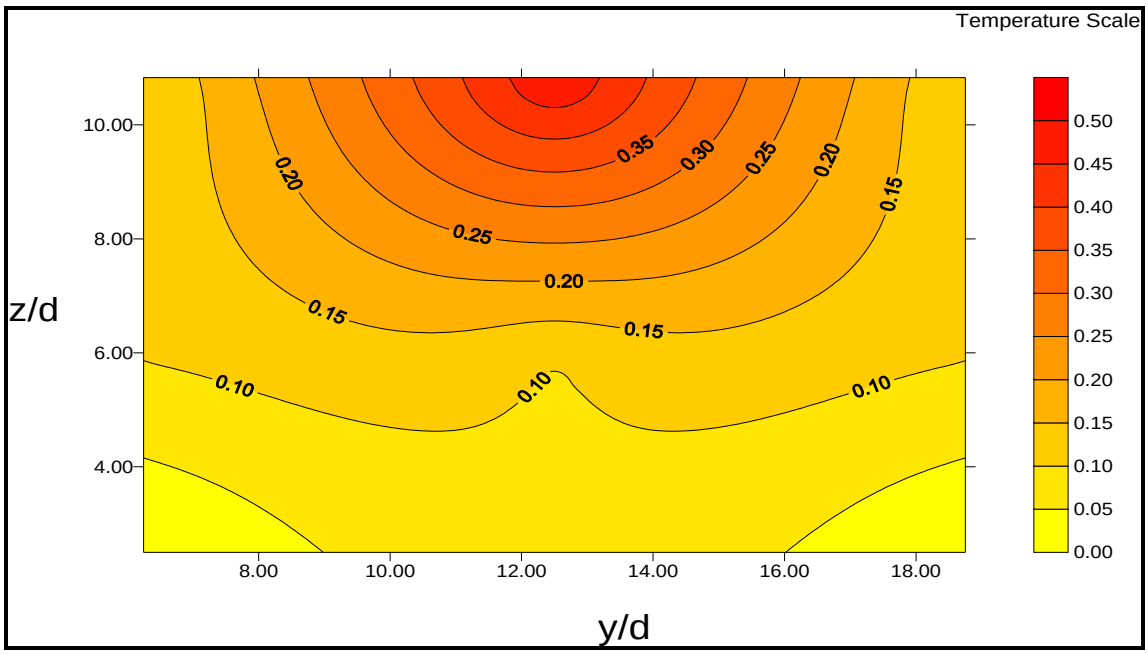

Figure 4.5a : Cross-sectional ΔT (in ^{0}C) at x/d = 110 for Q_a = 20.0 liter/s and Q_e = 0.05 liter/s.

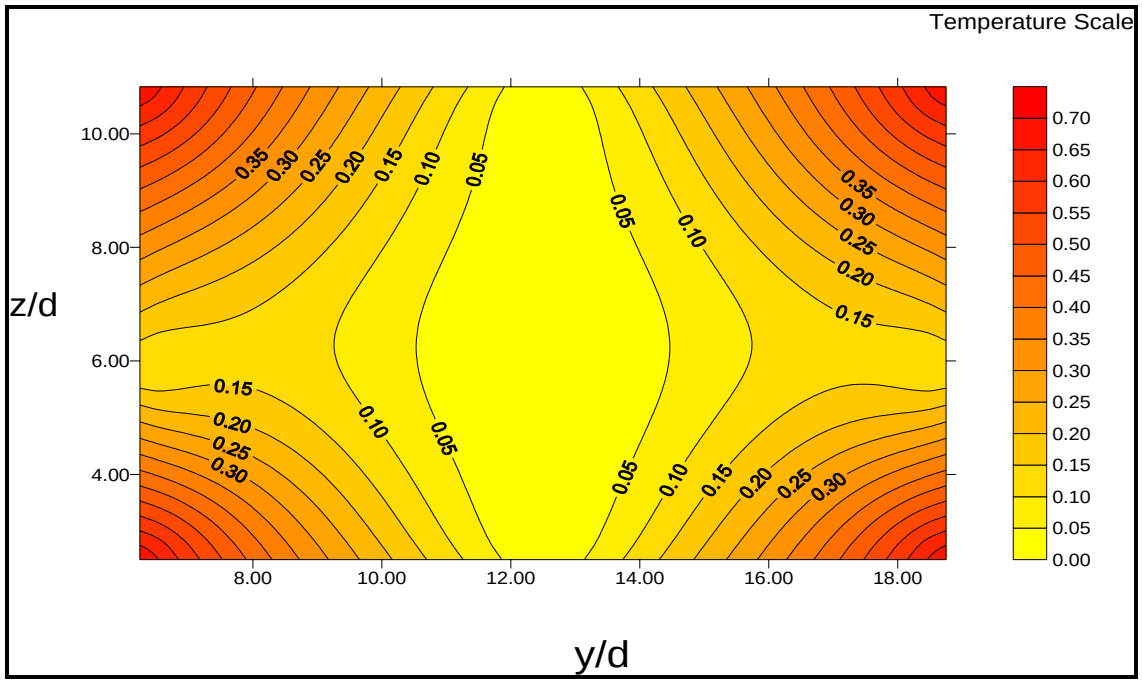

Figure 4.5b : Cross-sectional ΔT (in ^{0}C) at x/d = 110 for Q_a = 20.0 liter/s for Q_e of 0.133 liter/s.

Consequently, in Figure 4.5b, the highest temperature difference is 0.7 ^{0}C at both sides corners of the channel while the lowest temperature difference is 0 ^{0}C in the middle of the channel. At the centre of the flume, the velocity is higher compared to at the side of the flume. As a result, the mixing process at the centre of the flume is completed. The mixing by the flume wall is still incomplete as the velocity is smaller. This is caused by the mixing in this area is influenced by friction effect between the heated effluents with the side of the channel.

Meanwhile Figures 4.6a and 4.6b show isothermal lines to visualise the thermal effluent dispersion for ambient flow rate of 10 liter/s at x/d = 110 for Q_e of 0.05 liter/s and Q_e of 0.133 liter/s, respectively. Both figures show that mixing process at that station is almost complete. The highest temperature difference in Figure 4.6a is 1.0^{0}C while the lowest temperature difference is 0 ^{0}C at both sides of the channel. Referring Figure 4.6b, the highest temperature difference is 1.4 ^{0}C while the lowest temperature difference is 0 ^{0}C. From observation, the result shows that positive buoyancy has influenced the dispersion .

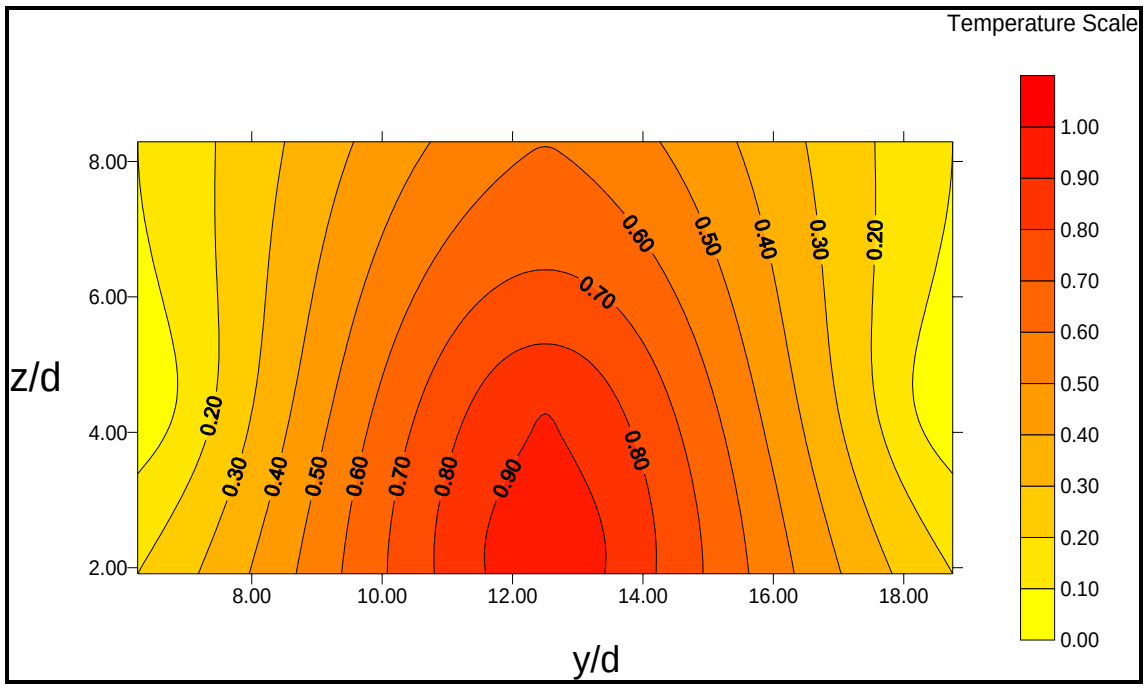

Figure 4.6a : Cross-sectional ΔT (in ^{0}C) at x/d = 110 for Q_a = 10.0 liter/s and Q_e = 0.05 liter/s

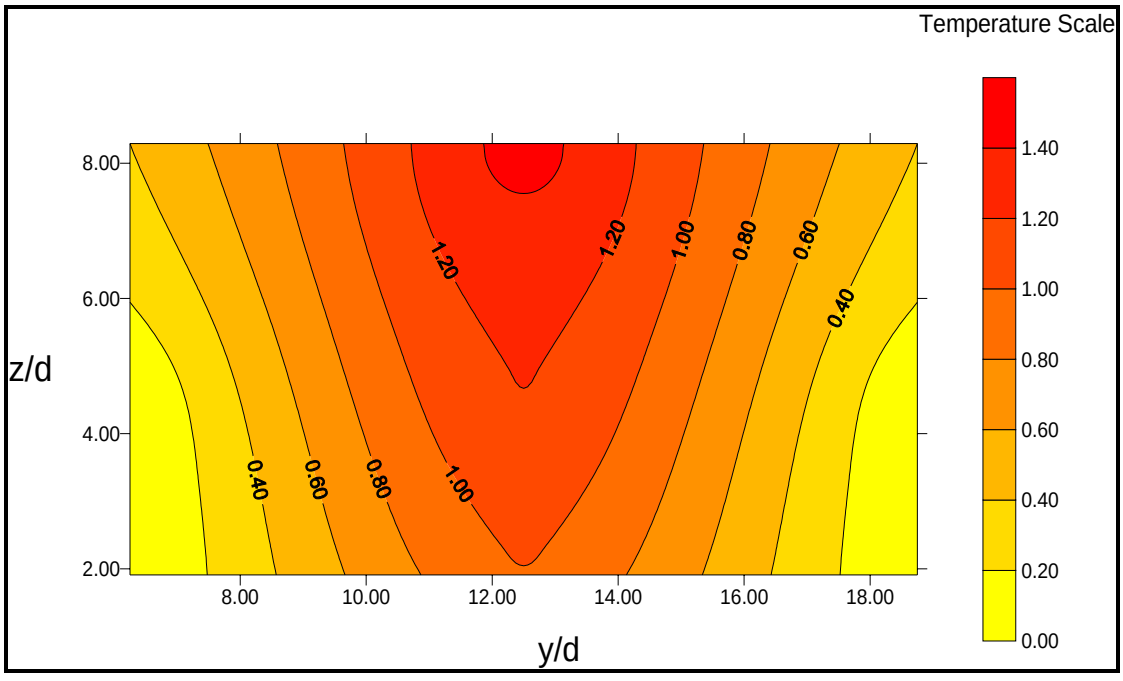

Figure 4.6b : Cross-sectional ΔT (in ^{0}C) at x/d = 110 for Q_a = 10.0 liter/s and Q_e = 0.133 liter/s.

Based on the observation of cross-sectional temperature differences in the channel, some conclusions can be made. The dispersion of thermal effluent in high ambient flow rate is higher due to its high velocity. Meanwhile, for larger volume of thermal effluent discharged, the dispersion rate is lower. This occurs due to the longitudinal distance needed in cooling the thermal effluent is longer. The difference in density between the ambient flow and thermal effluent discharge creates thermal stratification in the open channel flow.

4.6 Excess Temperature, $\Delta T/T_e$

Analysis on the temperature difference, ΔT is concentrated on two different ambient flow rates, Q_a of 20.0 liter/s and 10.0 liter/s and two different thermal effluent flow rates, Q_e of 0.133 liter/s and 0.05 liter/s. The ratio between the thermal effluent flow rates is 2.67. Subsequently, ΔT obtained in the analysis is normalised to acquire excess temperature, $\Delta T/T_e$ as in equation 2.10.

The study of excess temperature is carried out in three different flow depths known as lower layer, middle layer and upper layers. Lower layer of the flow represents z/H of 0.2 while middle layer corresponds to z/H of 0.4. The upper layer stands for z/H of 0.8.

4.6.1 Effect of Different Q_e on Excess Temperature for A Constant Q_a of 20 liter/s

Figure 4.7 shows longitudinal excess temperature profile for Q_a of 20 liter/s at lower layer of flow. At x/d of 0, for Q_e of 0.05 liter/s and Q_e of 0.133 liter/s, excess temperature is high as the thermometer detects the mass of heated water discharged into the channel. Then, excess temperature decreases since thermal effluent is cooling as it moves along the channel. This phenomenon arises as mixing occurs between thermal effluent and ambient flow. However, excess temperature for Q_e of 0.133 liter/s is high as the mass of thermal effluent discharge is higher compared to Q_e of 0.05 liter/s. The excess temperature equations for Q_e of 0.05 liter/s and Q_e of 0.133 liter/s at lower layer of flow are as follow respectively :

$$\frac{\Delta T}{T_e} = 1.285 \times 10^{-6} \left(\frac{x}{d}\right)^2 - 2.62 \times 10^{-4} \left(\frac{x}{d}\right) + 17.908 \times 10^{-3} \qquad (4.1)$$

$$\frac{\Delta T}{T_e} = 1.138 \times 10^{-6} \left(\frac{x}{d}\right)^2 - 2.772 \times 10^{-4} \left(\frac{x}{d}\right) + 18.565 \times 10^{-3} \qquad (4.2)$$

Figure 4.8 shows longitudinal excess temperature profile for Q_a of 20 liter/s at middle layer of flow. For Q_e of 0.05 liter/s, at x/d of 0, excess temperature is low with zero value because the thermometer does not detect the mass of heated water. However, as thermal effluent moves further downstream, excess temperature increases indicates that mass of thermal effluent moves upwards. The rising of thermal effluent in the receiving water is known as positive buoyancy. Afterward, excess temperature decreases along the channel length as the mixing between thermal effluent and ambient flow continue to take place. Equation 4.3 shows excess temperature for Q_e of 0.05 liter/s at middle layer of flow for Q_a of 20 liter/s.

$$\frac{\Delta T}{T_e} = -1.293 \times 10^{-6} \left(\frac{x}{d}\right)^2 + 1.872 \times 10^{-4} \left(\frac{x}{d}\right) + 2.171 \times 10^{-3} \qquad (4.3)$$

For Q_e of 0.133 liter/s, at x/d of 0, excess temperature is low because the thermometer does not detect the mass of heated water. However, as thermal effluent moves further downstream, excess temperature increases. Excess temperatures continue to increase due to large quantity of thermal effluent discharges in the channel. The excess temperature equation for Q_e of 0.133 liter/s at upper layer of flow is as shown in equation 4.4.

$$\frac{\Delta T}{T_e} = -2.305 \times 10^{-7}\left(\frac{x}{d}\right)^2 + 86.295 \times 10^{-6}\left(\frac{x}{d}\right) + 6.492 \times 10^{-4} \qquad (4.4)$$

Figure 4.9 shows longitudinal excess temperature profile for Q_a of 20 liter/s at upper layer of flow. For Q_e of 0.05 liter/s, at x/d of 0, excess temperature is low because the thermometer does not detect the mass of heated water as the heated water mass still flow at the lower layer of the flow. However, as thermal effluent move further, excess temperature increases. The tendency of thermal effluent to rise in the receiving water is generated by the density gradient. The fluctuation of data for Q_e of 0.05 liter/s is mainly caused by the turbulent flow of the ambient. Equation 4.5 shows excess temperature for Q_e of 0.05 liter/s at upper layer of flow for Q_a of 20 liter/s.

$$\frac{\Delta T}{T_e} = -4.004 \times 10^{-7}\left(\frac{x}{d}\right)^2 + 1.005 \times 10^{-4}\left(\frac{x}{d}\right) + 5.197 \times 10^{-3} \qquad (4.5)$$

At x/d of 0, for Q_e of 0.133 liter/s, excess temperature is low because the thermometer does not detect the mass of heated water as mentioned earlier for Q_e of 0.05 liter/s. However, as thermal effluent move further downstream, excess temperature increases to show mass of heated water moves upwards. Again, positive buoyancy plays a role where the thermal effluent rises upward in the receiving water. Excess temperature continues to increase due to the large quantity of thermal effluent discharged into the channel. The fluctuation of excess temperature for Q_e of 0.133 liter/s shows the presence of turbulence flow in the channel. The following equation 4.6

illustrates excess temperature for Q_e of 0.133 liter/s at upper layer of flow for Q_a of 20 liter/s.

$$\frac{\Delta T}{T_e} = -1.401 \times 10^{-6}\left(\frac{x}{d}\right)^2 + 3.197 \times 10^{-4}\left(\frac{x}{d}\right) + 2.894 \times 10^{-3} \qquad (4.6)$$

As a conclusion, when thermal effluent is discharged in the channel with high ambient flow rate, lower layer of the flow experienced the highest excess temperature since thermal effluent is submerged discharged from the bottom of the channel for both thermal effluent flow rates. However, the excess temperatures are low for middle and upper layer of the flow. Excess temperatures for larger effluent flow rates are higher compared to smaller effluent flow rates.

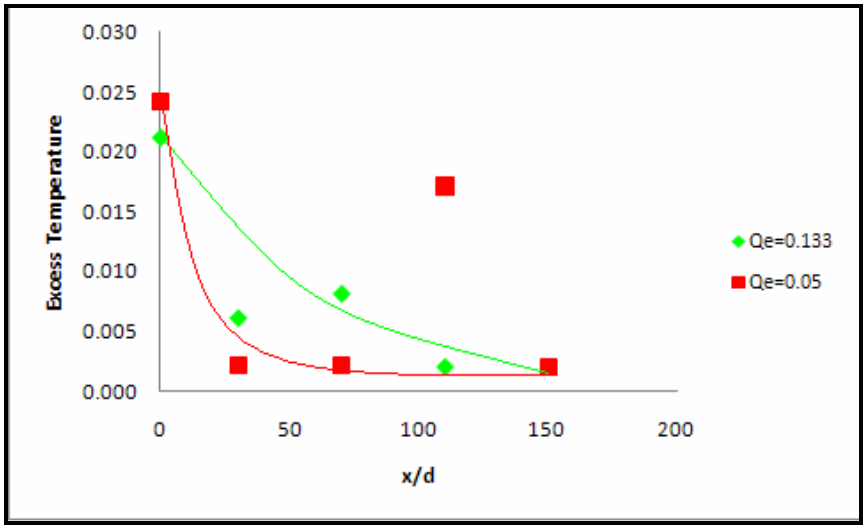

Figure 4.7: Longitudinal excess temperature profile, $\Delta T/T_e$ for Q_a of 20.0 liter/s at lower layer of flow for different Q_e.

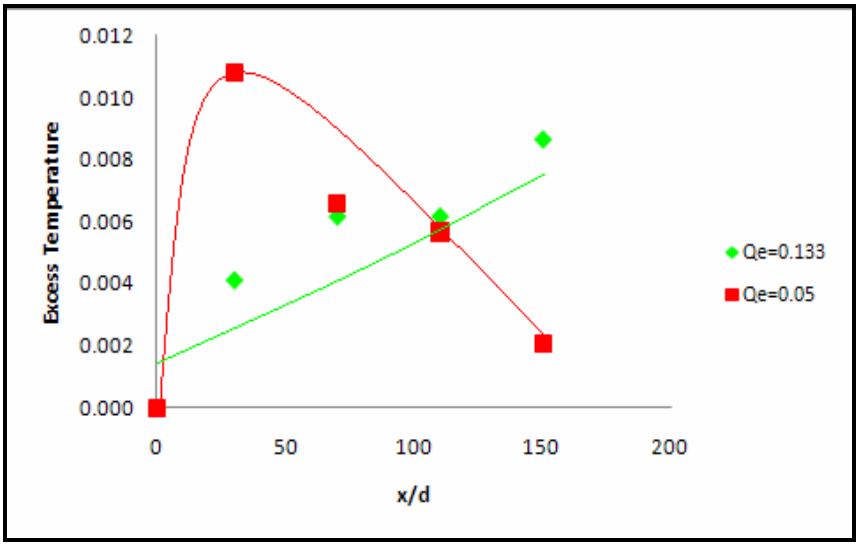

Figure 4.8 : Longitudinal excess temperature profile, $\Delta T/T_e$ for Q_a of 20.0 liter/s at middle layer of flow for different Q_e.

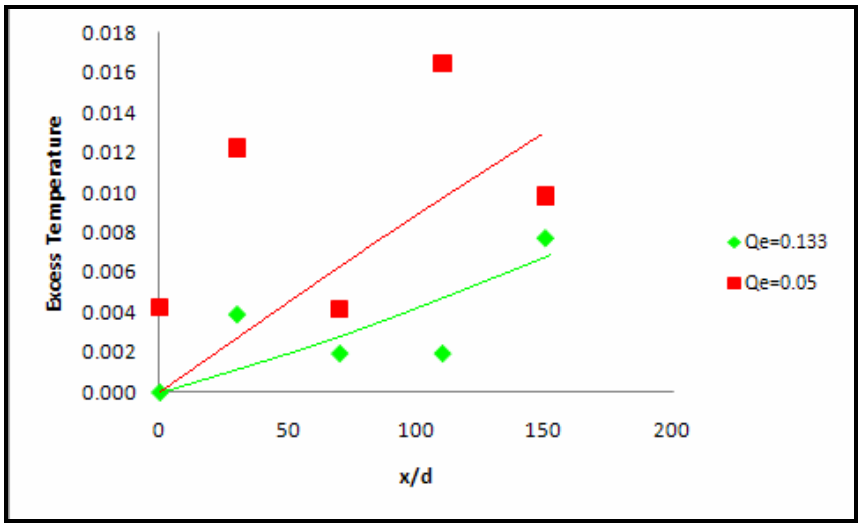

Figure 4.9 : Longitudinal excess temperature profile, $\Delta T/T_e$ for Q_a of 20.0 liter/s at upper layer of flow for different Q_e.

4.6.2 Effect of Different Q_e on Excess Temperature for A Constant Q_a of 10 liter/s

Figure 4.10 shows longitudinal excess temperature profile for Q_a of 10 liter/s at lower layer of flow. For Q_e of 0.05 liter/s and 0.133 liter/s, at x/d of 0, excess temperature is high because thermometer detects the mass of heated water. Excess temperature decreases with channel length as mixing between thermal effluent and ambient flow occurs and reduces the water temperature. Equations 4.7 and 4.8 show excess temperature equations for Q_e of 0.05 liter/s and Q_e of 0.133 liter/s at lower layer of flow for Q_a of 10 liter/s.

$$\frac{\Delta T}{T_e} = 1.037 \times 10^{-6}\left(\frac{x}{d}\right)^2 - 2.42 \times 10^{-4}\left(\frac{x}{d}\right) + 0.024 \qquad (4.7)$$

$$\frac{\Delta T}{T_e} = -2.88 \times 10^{-7}\left(\frac{x}{d}\right)^2 - 41.291 \times 10^{-6}\left(\frac{x}{d}\right) + 18.5 \times 10^{-3} \qquad (4.8)$$

Figure 4.11 shows longitudinal excess temperature profile for Q_a of 10 liter/s at middle layer of flow. For Q_e of 0.05 liter/s and 0.133 liter/s, at x/d of 0, excess temperature is high as the thermometer detected the mass of heated water. Excess temperature decreases with channel length as mixing occurs that reduced the water temperature. Excess temperature equations for Q_e of 0.05 liter/s and Q_e of 0.133 liter/s at middle layer of flow are as follow respectively:

$$\frac{\Delta T}{T_e} = 2.58 \times 10^{-6}\left(\frac{x}{d}\right)^2 - 5.909 \times 10^{-4}\left(\frac{x}{d}\right) + 0.037 \qquad (4.9)$$

$$\frac{\Delta T}{T_e} = -1.401 \times 10^{-6}\left(\frac{x}{d}\right)^2 + 3.197 \times 10^{-4}\left(\frac{x}{d}\right) + 16.79 \times 10^{-3} \qquad (4.10)$$

Figure 4.12 shows longitudinal excess temperature profile for Q_a of 10 liter/s at upper layer of flow. For Q_e of 0.05 liter/s, at x/d of 0, excess temperature is low with

zero value as the thermometer does not detect the mass of heated water. However, as thermal effluent moves further downstream, excess temperature increases that shows thermal effluent moves upwards. Again, the tendency of thermal effluent to rise in the receiving water is known as positive buoyancy. Equation of excess temperature for Q_e of 0.05 liter/s at upper layer of flow is as follow:

$$\frac{\Delta T}{T_e} = -1.249 \times 10^{-6} \left(\frac{x}{d}\right)^2 + 2.244 \times 10^{-4} \left(\frac{x}{d}\right) - 2.634 \times 10^{-4} \qquad (4.11)$$

For Q_e of 0.133 liter/s, at x/d of 0, excess temperature is low with zero value because the thermometer does not detect the mass of heated water. However, as thermal effluent move further downstream, excess temperature increases as the thermal effluent moves upwards. The excess continue to increase due to the large mass of thermal effluent discharges into the channel. Equation 4.12 shows excess temperature equation for Q_e of 0.133 liter/s at upper layer of flow.

$$\frac{\Delta T}{T_e} = -1.401 \times 10^{-6} \left(\frac{x}{d}\right)^2 + 3.197 \times 10^{-4} \left(\frac{x}{d}\right) + 2.894 \times 10^{-3} \qquad (4.12)$$

Overall, in low ambient flow rate, as thermal effluent is discharged in the channel, lower layer of the flow experienced the highest excess temperature as thermal effluent is discharged at the bottom of the channel for both thermal effluent flow rates. However, the excess temperatures are low in middle and upper layers of the flow. Excess temperatures resulted from high effluent flow rates are larger compared to low thermal effluent flow rates.

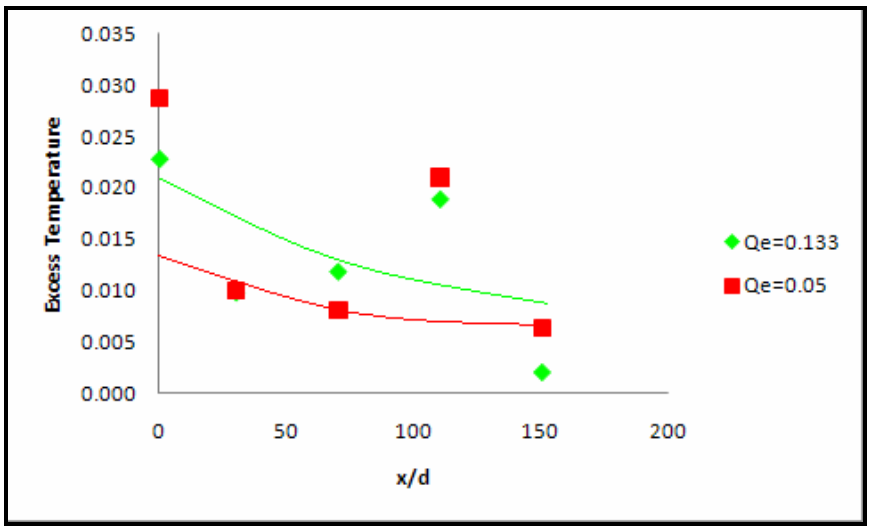

Figure 4.10 : Longitudinal excess temperature profile, $\Delta T/T_e$ for Q_a of 10.0 liter/s at lower layer of flow for different Q_e.

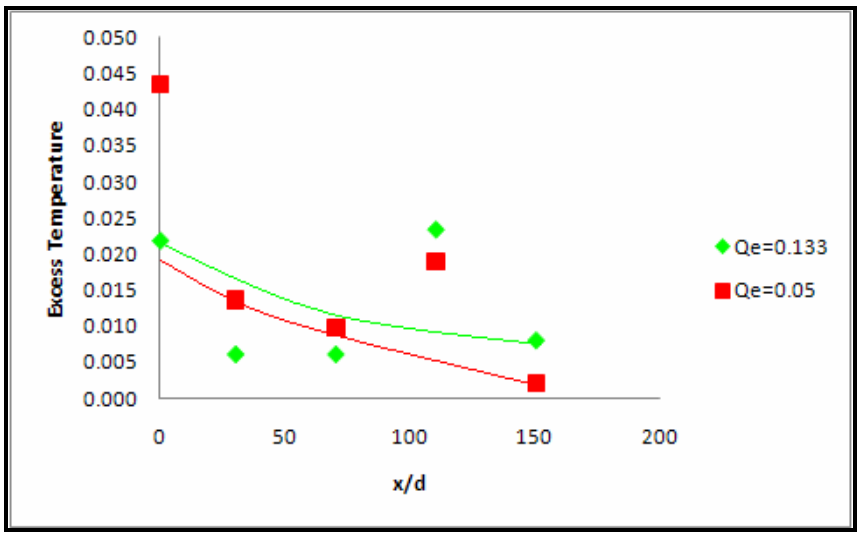

Figure 4.11 : Longitudinal excess temperature profile, $\Delta T/T_e$ for Q_a of 10.0 liter/s at middle layer of flow for different Q_e.

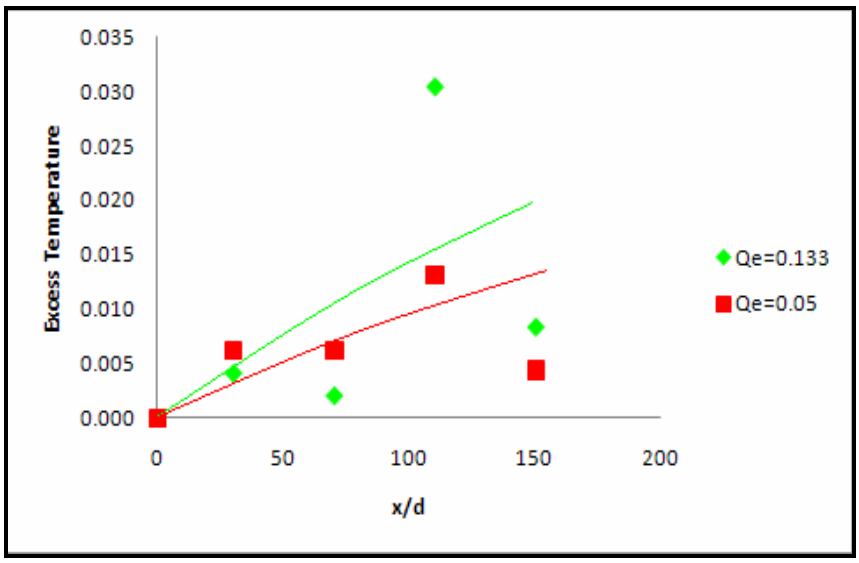

Figure 4.12 : Longitudinal excess temperature profile, $\Delta T/T_e$ for Q_a of 10.0 liter/s at upper layer of flow for different Q_e.

4.6.3 Effect of Different Q_a on Excess Temperature for A Constant Q_e of 0.133 liter/s

Figure 4.13 shows longitudinal excess temperature profile for Q_e of 0.133 liter/s at lower layer of flow. For Q_a of 20 liter/s and 10 liter/s, excess temperature is high because thermometer at x/d of 0 detects the mass of heated water. Excess temperature decreases along the channel length as mixing between thermal effluent and ambient flow takes place which reduces the water temperature.

Figure 4.14 shows longitudinal excess temperature profile for Q_e of 0.133 liter/s at middle layer of flow. For Q_a of 20 liter/s, excess temperature is low with zero value the mass of heated water is not detected by the thermometer. However, as thermal effluent moves further downstream, the excess temperature increases since the thermal

mass moves upwards. Excess temperatures keep increasing as a result of the large thermal effluent quantity discharged in the channel.

For Q_a of 10 liter/s, at x/d of 0, excess temperature is high as the thermometer detects the mass of heated water. Excess temperature decreases with channel length when mixing occurs between the ambient flow and the thermal effluent.

Figure 4.15 shows longitudinal excess temperature profile for Q_e of 0.133 liter/s at upper layer of flow. For Q_a of 20 liter/s and 10 liter/s, at x/d of 0, excess temperature is low because the thermometer does not detect the mass of heated water. However, as thermal effluent moves further, excess temperature increases as thermal effluent moves to the ambient flow surface. This behaviour of is known as positive buoyancy. Excess temperature continues to increase due to large quantity of thermal effluent discharged into the channel.

The analysis on effect of different Q_a on excess temperature for a constant high thermal effluent flow rate comes out with the following conclusion. In high thermal effluent flow rate, lower layer of the flow experiences the highest excess temperature since thermal effluent is discharged at the bottom of the channel for both ambient flow rates studied. However, the excess temperatures are low for middle and upper layer of the flow. Excess temperature for low ambient flow rate is higher compared to high ambient flow rates due to less volume of cold water to mix (cool) the heated water mass.

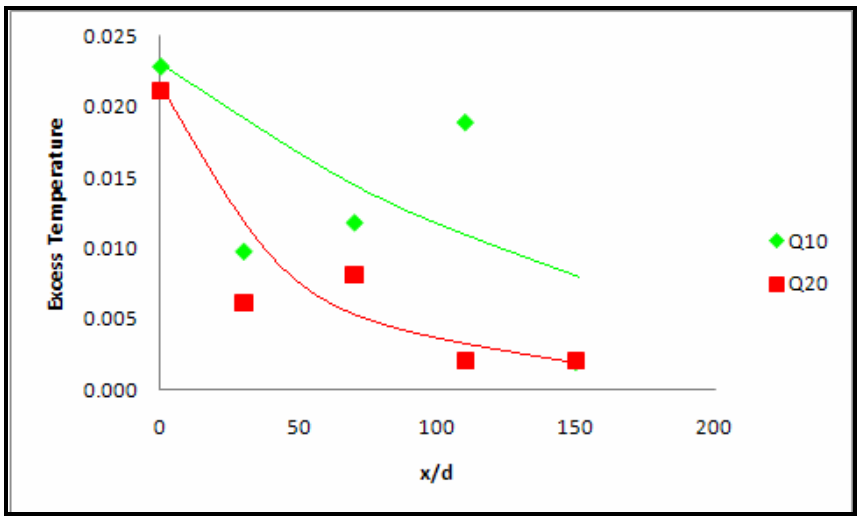

Figure 4.13 : Longitudinal excess temperature profile, $\Delta T/T_e$ for Q_e of 0.133 liter/s at lower layer of flow for different Q_a.

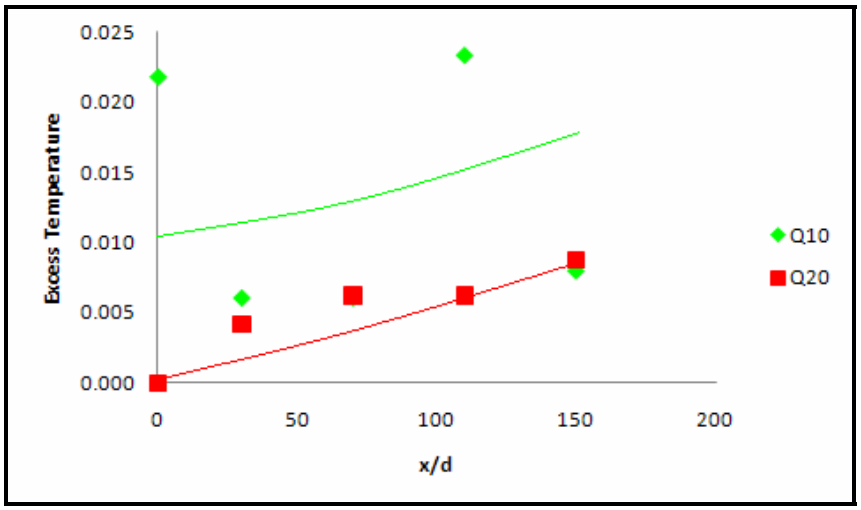

Figure 4.14 : Longitudinal excess temperature profile, $\Delta T/T_e$ for Q_e of 0.133 liter/s at middle layer of flow for different Q_a.

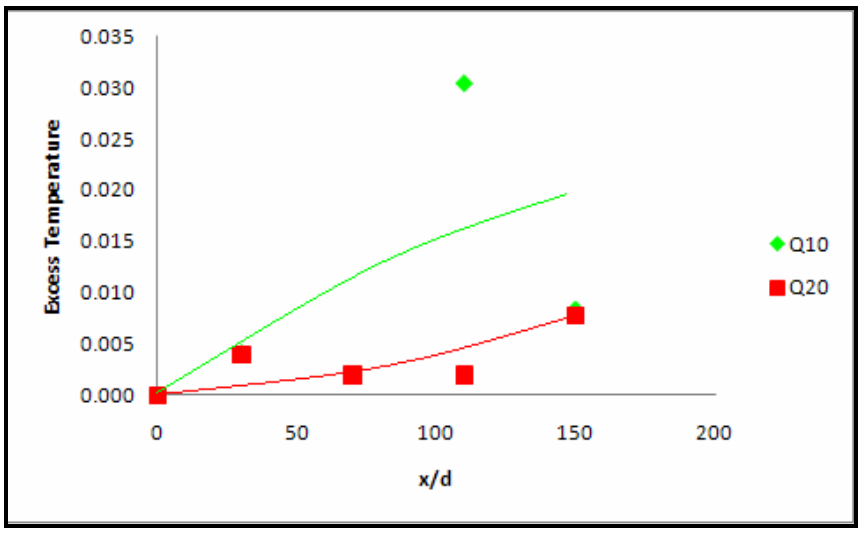

Figure 4.15 : Longitudinal excess temperature profile, $\Delta T/T_e$ for Q_e of 0.133 liter/s at upper layer of flow for different Q_a.

4.6.4 Effect of Different Q_a on Excess Temperature for A Constant Q_e of 0.05 liter/s

Figure 4.16 shows longitudinal excess temperature profile for Q_e of 0.05 liter/s at lower layer of flow. For Q_a of 20 liter/s and 10 liter/s, at x/d of 0, excess temperature is high because thermometer detects the mass of heated water. Excess temperature decreases with channel as mixing between thermal effluent and ambient flow occurs and reduces the water temperature.

Figure 4.17 shows longitudinal excess temperature profile for Q_e of 0.05 liter/s at middle layer of flow. For Q_a of 20 liter/s, at x/d of 0, excess temperature is low as the mass of heated water is not detected by the thermometer. However, as thermal effluent moves further, excess temperature increases as the thermal effluent moves upwards. Positive buoyancy is indicated by the rising of thermal effluent in the flume. Afterwards,

the excess temperature decreases with the channel length as mixing between thermal effluent and ambient flow occurs.

Meanwhile, for Q_a of 10 liter/s, at x/d of 0, excess temperature is high because thermometer detects the mass of heated water. Excess temperature decreases with channel length as mixing occurs between ambient flow and thermal effluent, thus reducing the water temperature.

Figure 4.18 shows longitudinal excess temperature profile for Q_e of 0.05 liter/s at upper layer of flow. For Q_a of 20 liter/s, at x/d of 0, excess temperature is low as the thermometer does not detect the mass of heated water. However, as thermal effluent moves further, excess temperature increases, signifying that the thermal effluent rises to the surface ambient flow. Excess temperature decreases in a region far from multi-port diffuser because mixing occurs between thermal effluent and ambient flow. The fluctuation of excess temperature shows that turbulent flow affected the mixing process.

For Q_a of 10 liter/s, at x/d of 0, excess temperature is low because the thermometer does not detect the mass of heated water. However, as thermal effluent moves further, excess temperature increases because the thermal effluent moves upwards due to the temperature gradient between thermal effluent discharged and ambient flow. Afterwards, excess temperature decreases because mixing between thermal effluent and ambient flow takes place.

In general, lower layer of the flow experiences the highest thermal impact due to the bottom discharges of effluent for both ambient flow rates in low thermal effluent flow rate. However, the excess temperatures are low for middle and upper layer of the

flow. Excess temperatures for low ambient flow rates are higher compared to high ambient flow rate due to less volume of cold water to cool the heated water mass.

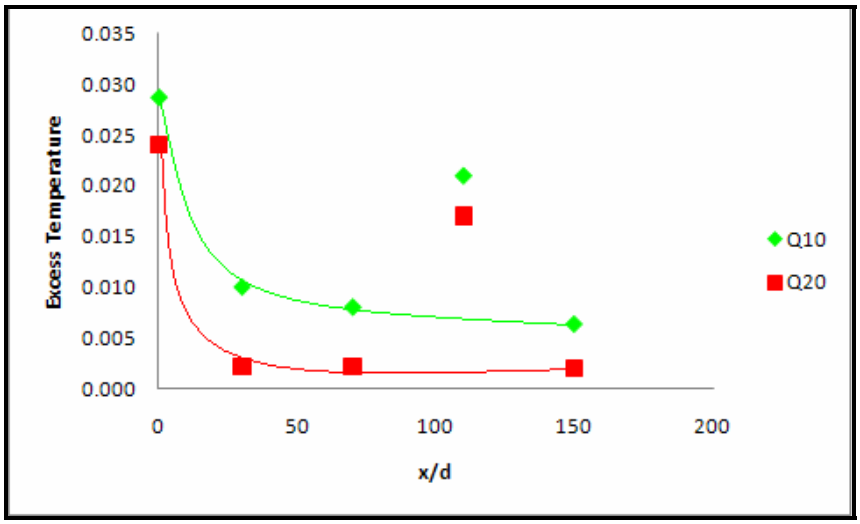

Figure 4.16 : Longitudinal excess temperature profile, $\Delta T/T_e$ for Q_e of 0.05 liter/s at lower layer of flow for different Q_a.

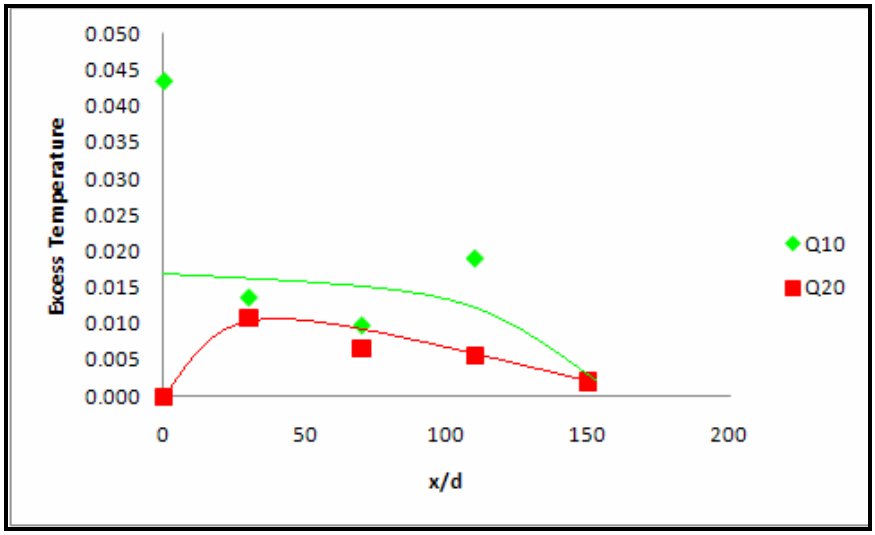

Figure 4.17 : Longitudinal excess temperature profile, $\Delta T/T_e$ for Q_e of 0.05 liter/s at middle layer of flow for different Q_a.

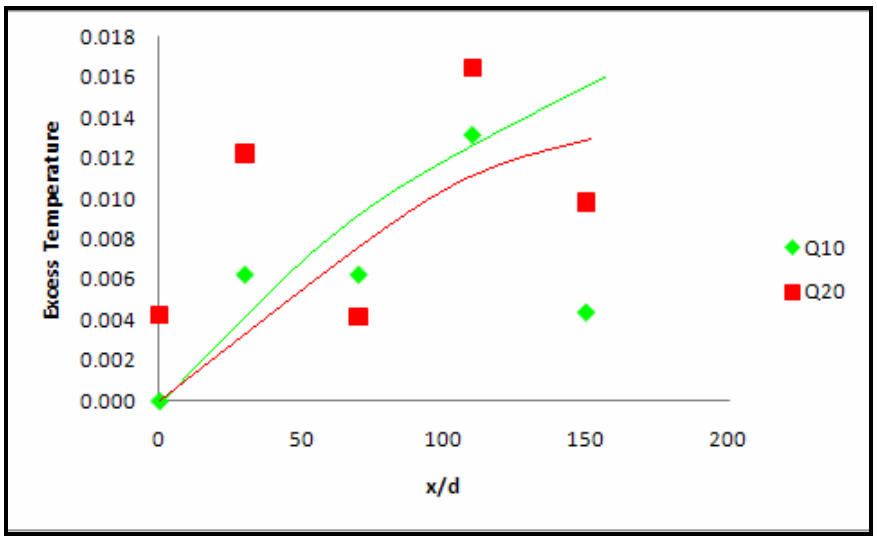

Figure 4.18 : Longitudinal excess temperature profile, $\Delta T/T_e$ for Q_e of 0.05 liter/s at upper layer of flow for different Q_a.

4.7 Dispersion Rate, K_T

Analysis on the effluent dispersion rate, K_T is important in determining the efficiency of pipe diffuser system in the experiment. Dispersion rate always inversely proportion to the excess temperature. A small changes of temperatures gives higher dispersion rates. Ambient flow velocity and distance from multiport diffuser influence dispersion rate in open channel. from K_T can be calculated using equation 2.11.

The analysis of dispersion rate is carried out three different flow depths known as lower layer, middle layer and upper layer of the flow. Lower layer of the flow represents the value z/H of 0.2 while middle layer corresponds to z/H of 0.4. Meanwhile, upper layer stands for z/H of 0.8.

The profile of calculated K_T is plotted along the channel and the results are discussed in the following sections.

4.7.1 Effect of Different Q_e on Dispersion Rate for A Constant Q_a of 20 liter/s

Figure 4.19 shows longitudinal dispersion rate profile for Q_a of 20 liter/s at lower layer of flow. For Q_e of 0.05 liter/s and 0.133 liter/s, as the excess temperature decreases along the channel length, the momentum ratio between ambient flow and thermal effluent discharged increases. Momentum is defined as the product of the mass of a body and its velocity (L. Mott, 1990). Momentum ratio influences the rising of dispersion rate. The dispersion rate for Q_e of 0.05 liter/s are higher compared to dispersion rate for Q_e of 0.133 liter/s because the momentum ratio for Q_e of 0.05 liter/s is higher compared to momentum ratio for Q_e of 0.133 liter/s. The dispersion rate equations for Q_e of 0.05 liter/s and Q_e of 0.133 liter/s at lower layer of flow are as follow respectively:

$$K_T = -6.059 \times 10^{-4}\left(\frac{x}{d}\right)^2 + 1.403\left(\frac{x}{d}\right) + 76.774 \qquad (4.13)$$

$$K_T = 27.279 \times 10^{-4}\left(\frac{x}{d}\right)^2 + 1.081\left(\frac{x}{d}\right) + 22.304 \qquad (4.14)$$

Figure 4.20 shows longitudinal dispersion rate profile for Q_a of 20 liter/s at middle layer of flow. Again, for Q_e of 0.05 liter/s and 0.133 liter/s, the momentum ratio between ambient flow and thermal effluent discharged increases because the excess temperatures decreases along the channel length. Definition of momentum is the product of the mass of a body and its velocity. As momentum ratio increases, dispersion rate also increases. The dispersion rate for Q_e of 0.05 liter/s are higher compared to dispersion

rates for Q_e of 0.133 liter/s because the momentum ratio for Q_e of 0.05 liter/s is higher compared to momentum ratio for Q_e of 0.133 liter/s. Equations 4.15 and 4.16 show dispersion rate equations for Qe of 0.05 liter/s and 0.133 liter/s at middle layer of flow respectively.

$$K_T = 8.09 \times 10^{-3}\left(\frac{x}{d}\right)^2 - 52.216 \times 10^{-3}\left(\frac{x}{d}\right) + 13.696 \quad (4.15)$$

$$K_T = -10.801 \times 10^{-3}\left(\frac{x}{d}\right)^2 + 1.762\left(\frac{x}{d}\right) + 22.233 \quad (4.16)$$

Figure 4.21 shows longitudinal dispersion rate profile for Q_a of 20 liter/s at upper layer of flow. For Q_e of 0.05 liter/s and 0.133 liter/s, as the excess temperatures increases along the channel length, the momentum ratio between ambient flow and thermal effluent discharged decreases. Momentum is the product of the mass of a body and its velocity. The decreasing of momentum ratio influenced the decreasing of dispersion rate. The dispersion rates for Q_e of 0.05 liter/s are lower compared to dispersion rates for Q_e of 0.133 liter/s due to turbulence generated by strong velocity of the jet discharged from the diffuser. The dispersion rate equations for Q_e of 0.05 liter/s and Q_e of 0.133 liter/s at lower layer of flow for Q_a of 20 liter/s are as follow:

$$K_T = 8.092 \times 10^{-4}\left(\frac{x}{d}\right)^2 - 0.448\left(\frac{x}{d}\right) + 89.926 \quad (4.17)$$

$$K_T = -31.96 \times 10^{-3}\left(\frac{x}{d}\right)^2 + 5.05\left(\frac{x}{d}\right) + 5.441 \quad (4.18)$$

Based on the analysis of effect of different Q_e on dispersion rate for a constant high ambient flow rate, the dispersion rates for lower thermal effluent flow rate are higher compared to higher thermal effluent flow rate in high ambient flow rate because the momentum ratio for lower thermal effluent flow rate is higher than momentum ratio for higher thermal effluent flow rate.

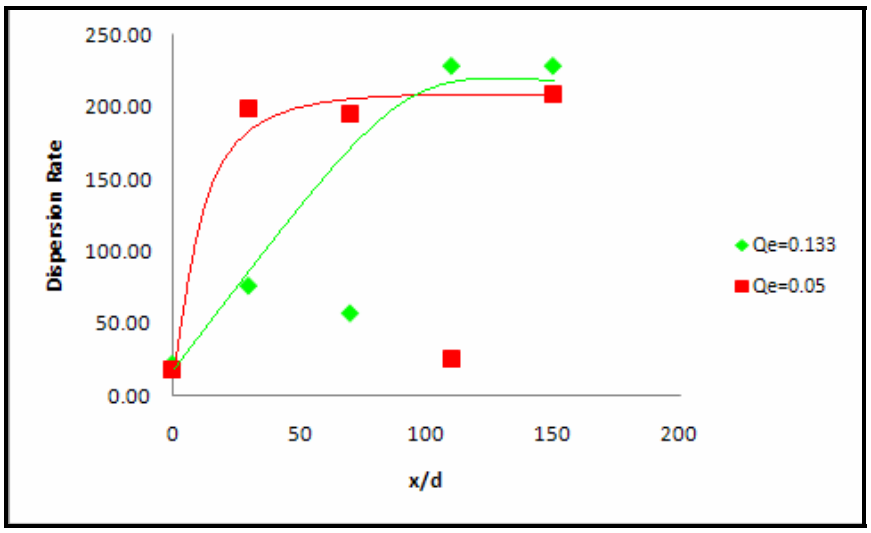

Figure 4.19 : Longitudinal dispersion rate profile, K_T for Q_a of 20.0 liter/s at lower layer of flow for different Q_e.

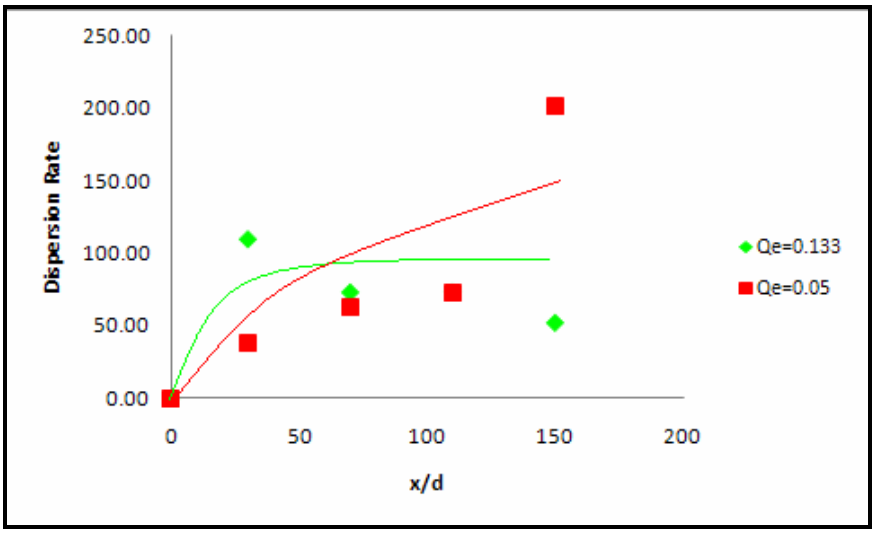

Figure 4.20 : Longitudinal dispersion rate profile, K_T for Q_a of 20.0 liter/s at middle layer of flow for different Q_e.

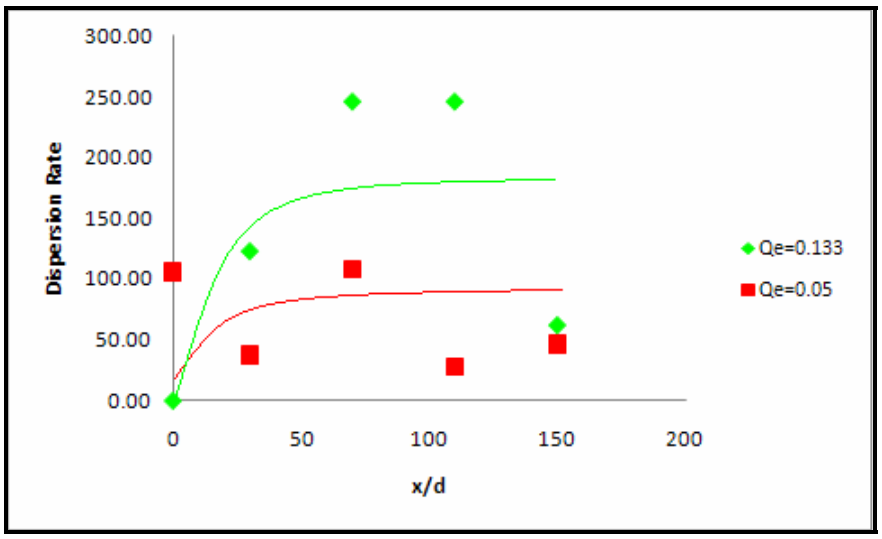

Figure 4.21 : Longitudinal dispersion rate profile, K_T for Q_a of 20.0 liter/s at upper layer of flow for different Q_e.

4.7.2 Effect of Different Q_e on Dispersion Rate for A Constant Q_a at 10 liter/s

Figure 4.22 shows longitudinal dispersion rate profile for Q_a of 10 liter/s at lower layer of flow. For Q_e of 0.05 liter/s and 0.133 liter/s, as the excess temperature decreases along the channel length, the momentum ratio increases. Momentum is the product of the mass of a body and its velocity. The rising of momentum ratio influence the rising of dispersion rate. The dispersion rate for Q_e of 0.05 liter/s are higher compared to dispersion rate for Q_e of 0.133 liter/s because the momentum ratio for Q_e of 0.05 liter/s is higher compared to momentum ratio for Q_e of 0.133 liter/s. The dispersion rate equations for Q_e of 0.05 liter/s and Q_e of 0.133 liter/s at lower layer of flow are as shown in equation 4.19 and 4.20 respectively.

$$K_T = -1.547 \times 10^{-3} \left(\frac{x}{d}\right)^2 + 0.526\left(\frac{x}{d}\right) + 12.503 \qquad (4.19)$$

$$K_T = 19.646 \times 10^{-3}\left(\frac{x}{d}\right)^2 - 1.811\left(\frac{x}{d}\right) + 47.479 \quad (4.20)$$

Figure 4.23 shows longitudinal dispersion rate profile for Q_a of 10 liter/s at middle layer of flow. For Q_e of 0.05 liter/s and 0.133 liter/s, as the excess temperatures decreases along the channel length, the momentum ratio increases. Momentum ratio is proportional to dispersion rate. The rising of momentum ratio influence the rising of dispersion rate. The dispersion rate for Q_e of 0.05 liter/s are higher compared to dispersion rate for Q_e of 0.133 liter/s because the momentum ratio for Q_e of 0.05 liter/s is higher compared to momentum ratio for Q_e of 0.133 liter/s. The dispersion rate equations for Q_e of 0.05 liter/s and Q_e of 0.133 liter/s at lower layer of flow for Q_a of 10 liter/s are as follow:

$$K_T = 2.58 \times 10^{-6}\left(\frac{x}{d}\right)^2 - 5.909 \times 10^{-4}\left(\frac{x}{d}\right) + 0.037 \quad (4.21)$$

$$K_T = -4.037 \times 10^{-3}\left(\frac{x}{d}\right)^2 + 0.63\left(\frac{x}{d}\right) + 38.283 \quad (4.22)$$

Figure 4.24 shows longitudinal dispersion rate profile for Q_a of 10 liter/s at upper layer of flow. For Q_e of 0.05 liter/s and 0.133 liter/s, as the excess temperature decreases along the channel length, the momentum ratio increases. Momentum is the product of the mass of a body and its velocity. Again, the rising of momentum ratio influence the rising of dispersion rate. The dispersion rate for Q_e of 0.05 liter/s are lower compared to dispersion rate for Q_e of 0.133 liter/s due to turbulence generated by strong velocity of the jet discharged from the diffuser. Equations 4.23 and 4.24 show dispersion rate equations for Q_e of 0.05 liter/s and Q_e of 0.133 liter/s at upper layer of the flow.

$$K_T = -1.249 \times 10^{-6}\left(\frac{x}{d}\right)^2 + 2.244 \times 10^{-4}\left(\frac{x}{d}\right) - 2.634 \times 10^{-4} \quad (4.23)$$

$$K_T = -22.477 \times 10^{-3}\left(\frac{x}{d}\right)^2 + 3.346\left(\frac{x}{d}\right) + 19.44 \qquad (4.24)$$

As a conclusion, in low ambient flow rate, as thermal effluent is discharged in the channel, the dispersion rate for lower thermal effluent flow rate are higher compared to dispersion rate for higher thermal effluent flow rate because the momentum ratio for lower thermal effluent flow rate is higher compared to momentum ratio for higher thermal effluent flow rate.

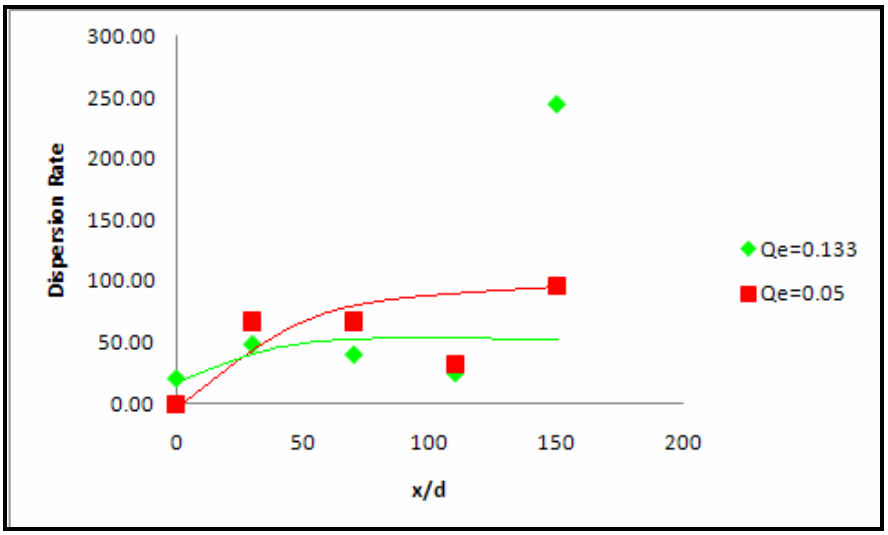

Figure 4.22 : Longitudinal dispersion rate profile, K_T for Q_a of 10.0 liter/s at lower layer of flow for different Q_e.

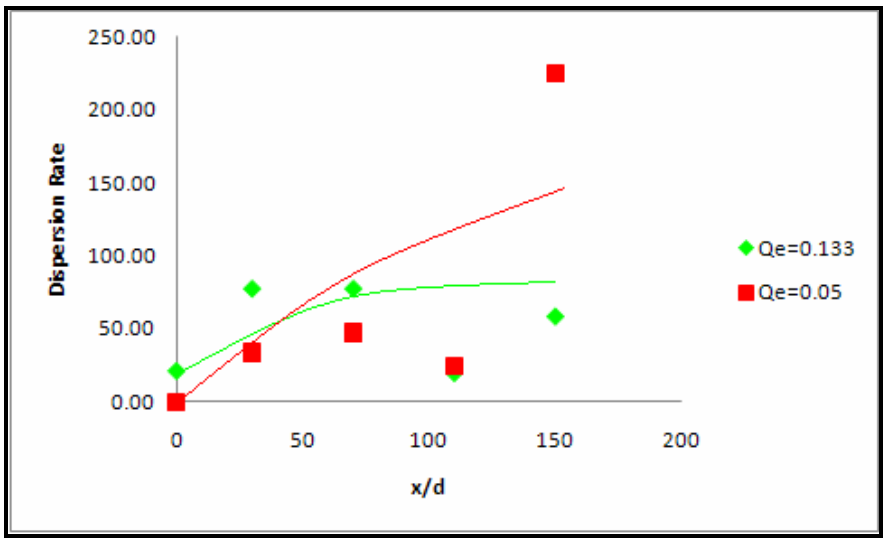

Figure 4.23 : Longitudinal dispersion rate profile, K_T for Q_a of 10.0 liter/s at middle layer of flow for different Q_e.

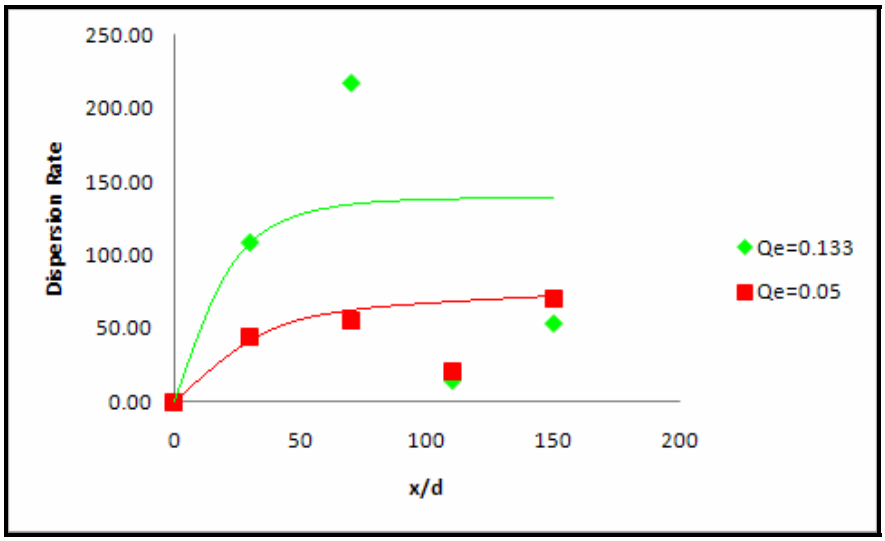

Figure 4.24 : Longitudinal dispersion rate profile, K_T for Q_a of 10.0 liter/s at upper layer of flow for different Q_e.

4.7.3 Effect of Different Q_a on Dispersion Rate for A Constant Q_e at 0.133 liter/s

Figure 4.25 shows longitudinal dispersion rate profile for Q_e of 0.133 liter/s at lower layer of flow. For Q_a of 20 liter/s and 10 liter/s, as the excess temperature decreases along the channel length, the momentum ratio increases. Momentum is defined as the product of the mass of a body and its velocity. The rising of momentum ratio influence the rising of dispersion rates. The dispersion rate for Q_a of 20 liter/s is higher than dispersion rates for Q_a of 10 liter/s because the momentum ratio is higher than momentum ratio for Q_a of 10 liter/s.

Figure 4.26 shows longitudinal dispersion rate profile for Q_e of 0.133 liter/s at middle layer of flow. For Q_a of 20 liter/s and 10 liter/s, as the excess temperature decreases along the channel length, the momentum ratio increases. Momentum is the product of the mass of a body and its velocity. The rising of momentum ratio influence the rising of dispersion rate. The dispersion rates for Q_a of 20 liter/s are higher than dispersion rate for Q_a of 10 liter/s because the momentum ratio is higher than momentum ratio for Q_a of 10 liter/s.

Figure 4.27 shows longitudinal dispersion rate profile for Q_e of 0.133 liter/s at upper layer of flow. For Q_a of 20 liter/s and 10 liter/s, as the excess temperatures increases along the channel length, the momentum ratio decreases. The decreasing of momentum ratio influenced the decreasing of dispersion rates. The dispersion rate for Q_a of 20 liter/s are higher compared to dispersion rates for Q_a of 10 liter/s because the momentum ratio is higher compared to momentum ratio for Q_a of 10 liter/s.

In general, as thermal effluent is discharged in the channel, the dispersion rates for higher ambient flow rate are higher compared to dispersion rate for lower ambient

flow rate in high thermal effluent flow rate because the momentum ratio for higher ambient flow rate is higher compared to momentum ratio for lower ambient flow rate.

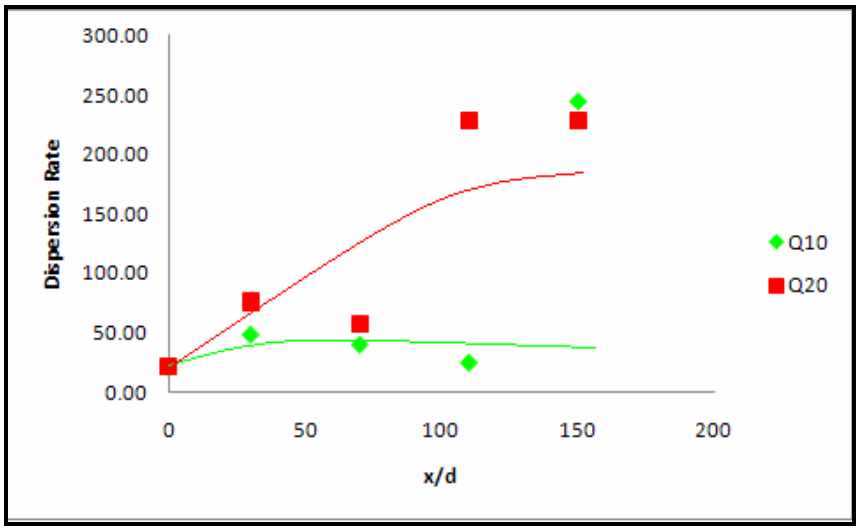

Figure 4.25 : Longitudinal dispersion rate profile, K_T for Q_e of 0.133 liter/s at lower layer of flow for different Q_a.

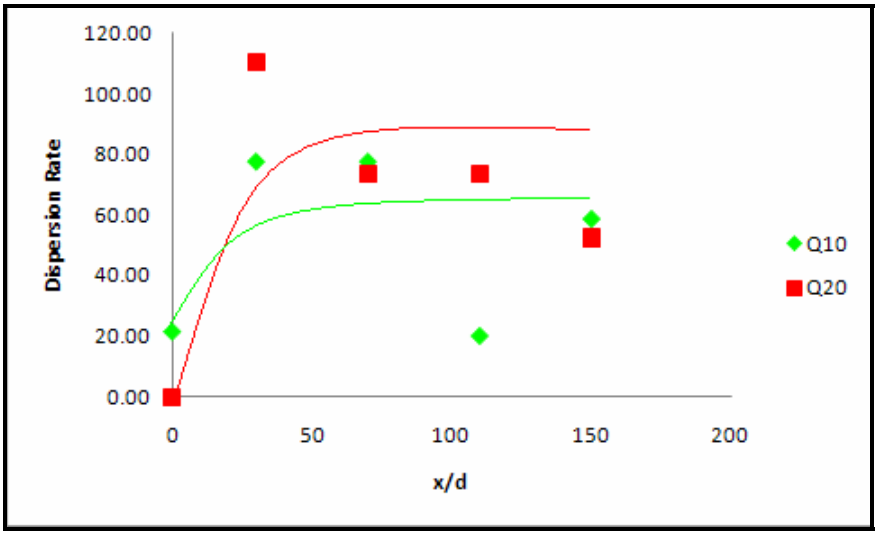

Figure 4.26 : Longitudinal dispersion rate profile, K_T for Q_e of 0.133 liter/s at middle layer of flow for different Q_a.

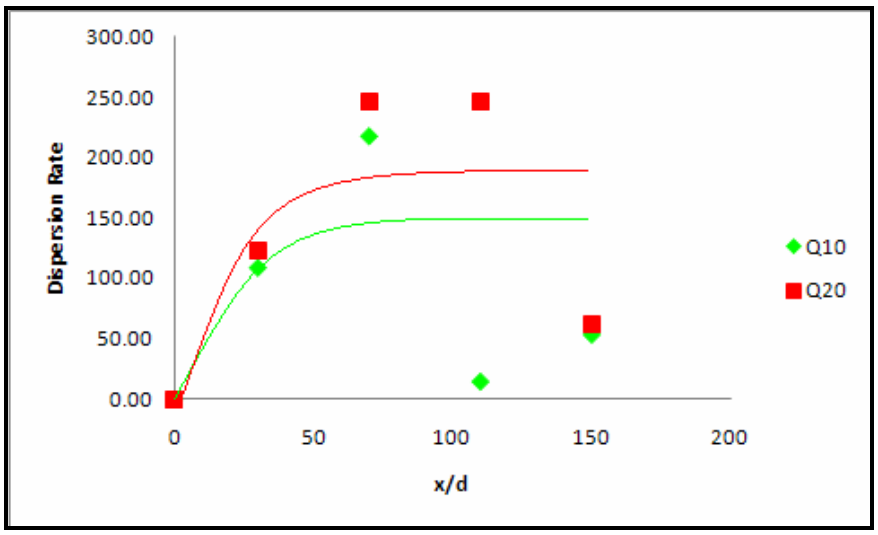

Figure 4.27 : Longitudinal dispersion rate profile, K_T for Q_e of 0.133 liter/s at upper layer of flow for different Q_a.

4.7.4 Effect of Different Q_a on Dispersion Rate for A Constant Q_e at 0.05 liter/s

Figure 4.28 shows longitudinal dispersion rate profile for Q_e of 0.05 liter/s at lower layer of flow. For Q_a of 20 liter/s and 10 liter/s, as the excess temperature decreases along the channel length, the momentum ratio increases. As momentum ratio is proportional to the dispersion rate, the rising of momentum ratio influences the rising of dispersion rate. The dispersion rate for Q_a of 20 liter/s is higher compared to dispersion rate for Q_a of 10 liter/s because the momentum ratio for Q_a of 20 liter/s is higher than momentum ratio for Q_a of 10 liter/s.

Figure 4.29 shows longitudinal dispersion rate profile for Q_e of 0.05 liter/s at middle layer of flow. Again, excess temperature is inversely proportional to the momentum ratio. As the excess temperature decreases along the channel length, the momentum ratio increases. The rising of momentum ratio influence the rising of

dispersion rate. Momentum is the product of the mass of a body and its velocity. The dispersion rate for Q_a of 20 liter/s is higher compared to dispersion rate for Q_a of 10 liter/s because the momentum ratio for Q_a of 20 liter/s is higher than momentum ratio for Q_a of 10 liter/s.

Figure 4.30 shows longitudinal dispersion rate profile for Q_e of 0.05 liter/s at upper layer of flow. As the excess temperatures increases along the channel length, the momentum ratio decreases. The decreasing of momentum ratio influenced the decreasing of dispersion rate. The dispersion rate for Q_a of 20 liter/s are higher compared to dispersion rate for Q_a of 10 liter/s because the momentum ratio for Q_a of 20 liter/s is higher compared to momentum ratio for Q_a of 10 liter/s.

Overall, in lower thermal effluent flow rate, as thermal effluent is discharged in the channel, the dispersion rate for higher ambient flow rate are higher compared to dispersion rate for lower ambient flow rate because the momentum ratio for higher ambient flow rate is higher compared to momentum ratio for lower ambient flow rate.

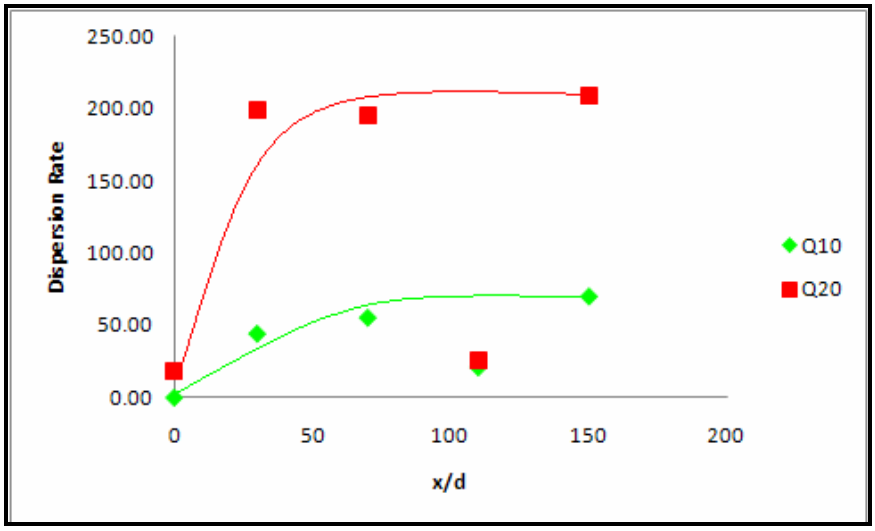

Figure 4.28 : Longitudinal dispersion rate profile, K_T for Q_e of 0.05 liter/s at lower layer of flow for different Q_a.

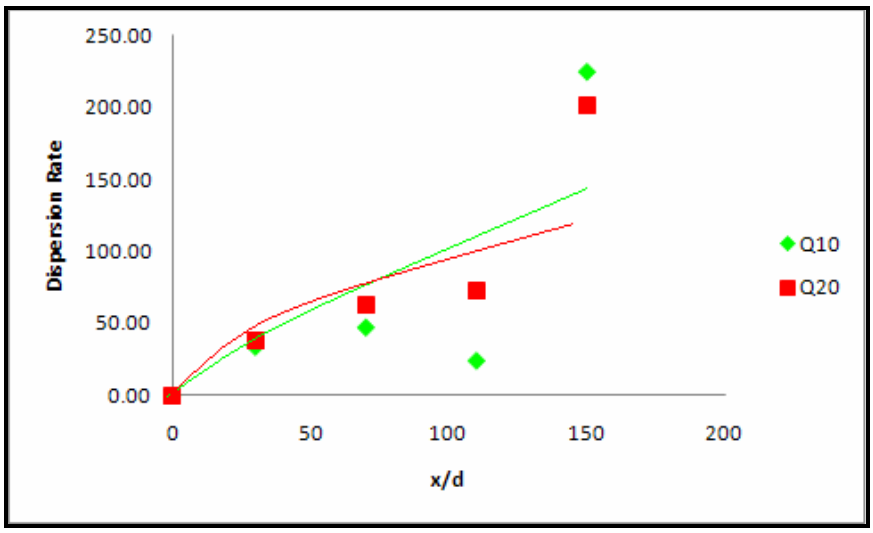

Figure 4.29 : Longitudinal dispersion rate profile, K_T for Q_e of 0.05 liter/s at middle layer of flow for different Q_a.

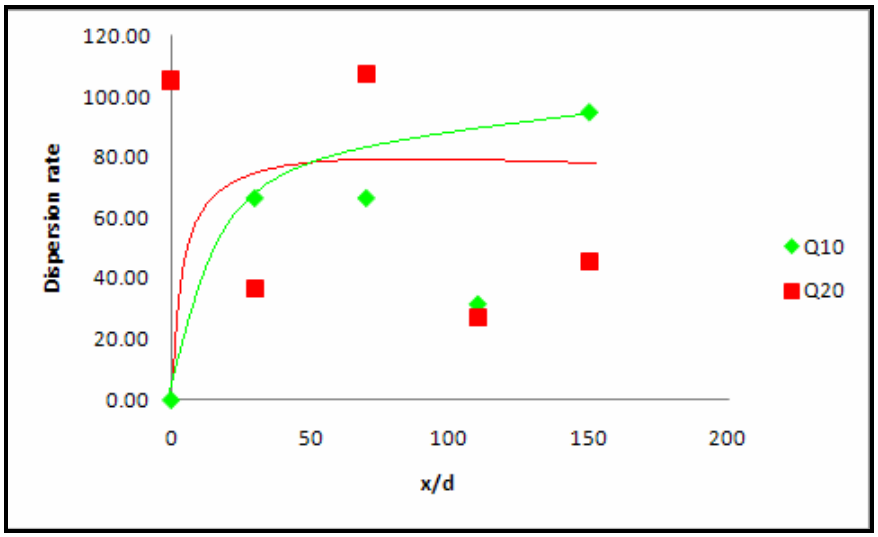

Figure 4.30 : Longitudinal dispersion rate profile, K_T for Q_e of 0.05 liter/s at upper layer of flow for different Q_a.

4.8 Ambient Temperature Differences, ΔT with Dimensionless Time, t*

Data of temperature difference, ΔT is obtained as discussed earlier. The dimensionless time, t* is used in the analysis in which t* is equal to:

$$t^* = \frac{t}{t_e} \tag{4.25}$$

where t is time recorded for the experiment while t_e is time taken to discharge thermal effluent into the channel which is 210 seconds.

Data is collected at x/d of 30 and x/d of 110 at three different flow depths, z/H of 0.2 (lower layer of the flow), z/H of 0.4 (middle layer of the flow) and z/H of 0.8 (upper layer of the flow). However, the discussion is focused on z/H of 0.4 and y/d of 12.5 for flow rates of 20.0 liter/s and 10.0 liter/s.

Based on Figure 4.31 for Q_a of 20 liter/s, maximum temperature difference recorded is 0.5 at x/d of 30 which is located in near-field region. This condition happens because station x/d of 30 is located near to the diffuser pipe and experiences the high temperature of heated water. At x/d of 110, heated water has mixed with ambient water therefore the maximum temperature difference is 0.26 lesser than temperature difference at x/d of 30. According to the Figure 4.32, when t* is larger than 1, the temperature difference decreases as no more heat is loaded to the water flow.

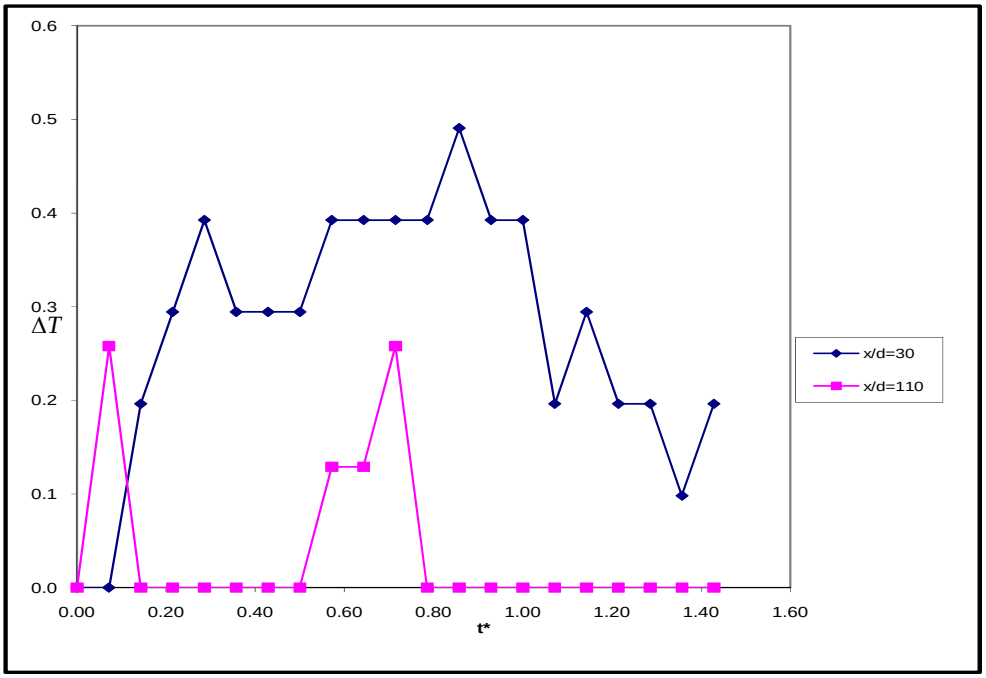

Figure 4.31 : Temporal changes on temperature difference for Q_a of 20 liter/s at x/d of 30 and x/d of 110

Based on Figure 4.32 for Q_a of 10 liter/s, maximum temperature difference is 0.68 at x/d of 30 which is located in near-field region. This condition happens because the station x/d of 30 is located near the diffuser pipe and experiences the high temperature of heated mass. At x/d of 110, heated water has mixed with ambient water therefore the maximum temperature difference is less than temperature difference at x/d of 30. According to the Figure 4.32, when t* is larger than 1, the temperature difference decreases as no more heat is loaded to the water flow. Maximum temperature difference recorded at x/d of 30 for Q_a of 10 liter/s is higher than Q_a of 20 liter/s because of the less ambient flow volume in the channel.

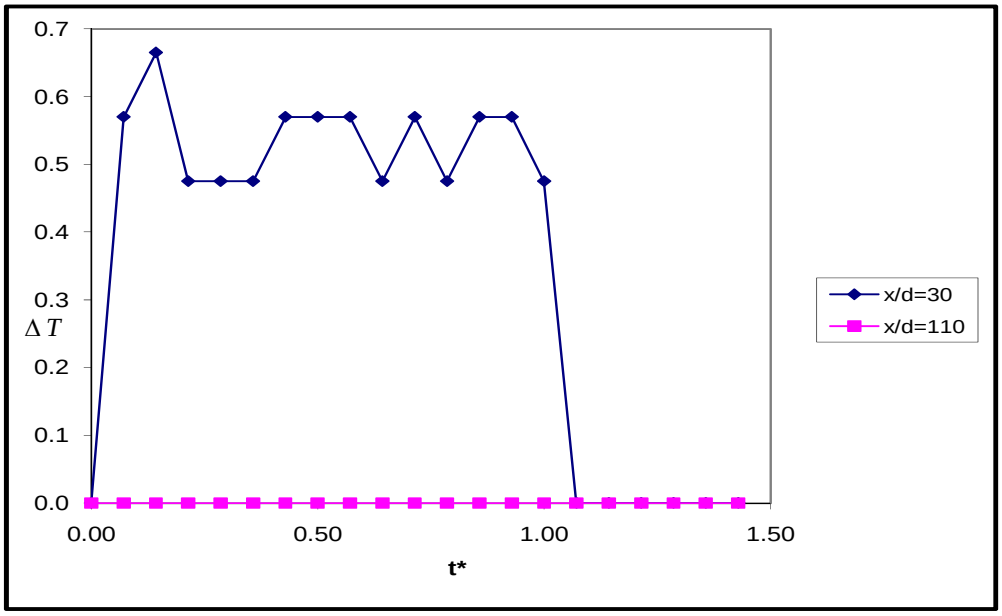

Figure 4.32 : Temporal changes on temperature difference for Q_a of 10 liter/s at x/d of 30 and x/d of 110

CHAPTER 5

CONCLUSION AND RECOMMENDATION

5.1 Conclusion

Experiment on thermal effluent discharge in open channel flow is a complex process since it is dealing with turbulence, density difference and heat loss in a water body. However, the research gives some basic understanding on the thermal effluent mixing process.

Based on the analysis in Chapter 4, conclusions that can be made from the investigation on behaviour of thermal effluent in free surface flow are as follow:

(i) Positive buoyancy occurs when thermal effluent is discharged into ambient flow at the bottom of the channel. The heated mass moves upward to the water surface as the density of heated water is lower than ambient water.

(ii) The thermal effluent disperses uniformly and cools gradually when it moves further from the discharge point.

(iii) The lower layer of flow experiences high excess temperature compared to middle and upper layer of the flow.

(iv) Larger effluent flow rate produces higher excess temperature in the receiving water body than small effluent flow rate.

(v) The lower ambient flow rate experiences higher excess temperature due to less volume of cold water to mix (cool) the heated water mass.

(vi) The dispersion rate for small thermal effluent flow rate is higher than dispersion rate for large thermal effluent flow rate. The momentum ratio for small thermal effluent flow rate is higher than momentum ratio for large thermal effluent flow rate.

(vii) The dispersion rate for higher ambient flow rate are higher compared to dispersion rate for lower ambient flow rate in high thermal effluent flow rate because the momentum ratio for higher ambient flow rate is higher compared to momentum ratio for lower ambient flow rate.

(viii) Some empirical equations are established on the profiles of excess temperature and dispersion rate along the channel.

5.2 Recommendations

Experiment on in open channel flow is a complex process since it is dealing with turbulence, density difference and heat loss in a water body. However, the research gives some basic understanding on the thermal effluent mixing process.

Based on the experiment that has been carried out, there are a few steps should be improved to produce better results in the upcoming experimental study. The following recommendations for the next experiment:

(i) Highly sensitive equipments especially digital thermometer is very important in the experimental research. However, this will increase the cost of the study

(ii) Surrounding environment must be controlled. For example, wind affects the water temperature in the flume.

(iii) Thermal effluent flow rate can be determined precisely using ultrasonic flowmeter. The equipment should be installed at multi-port diffuser pipe.

(iv) Digital thermometer is an important equipment in the laboratory experiment. Therefore, it should be calibrated prior to conduct the experiment in order to obtain accurate data.

(v) As an alternative to digital thermometer, data logger can be used as an effective temperature measurement device

The study on thermal effluent discharge in open channel flow can be further expanded. Among the identified topics suggested for future study are:

(i) The study on effect of turbulent on thermal effluent discharge in open channel flow,

(ii) The effect of diffuser pipe submergence on the excess temperature and dispersion rate profiles in free surface flow,

(iii) Changes of temperature profiles in receiving water due to different heated mass loads (effluent temperatures),

(iv) The study on behaviour of thermal effluent discharge in open channel with different aspect ratios,

(v) The study on thermal effluent discharge in compound channels, and

(vi) The study on thermal effluent discharge in straight and meandering channels.

APPENDIX A

Dimensional Analysis

Parameters that influenced the dispersion of thermal effluent in ambient flow:

i. ambient flow rate, Q_a [L^3T^{-1}]
ii. effluent flow rate, Q_e [L^3T^{-1}]
iii. temperature difference, T_x - T_a, ΔT (^0C)
iv. effluent temperature, T_e (^0C)
v. vertical distance from bed of channel, z [L]
vi. transverse distance from channel wall, y [L]
vii. longitudinal distance from channel wall, x [L]
viii. cross-section area of the channel, A [L^2]
ix. width of the channel, B [L]
x. diameter of port, d [L]
xi. horizontal distance from discharge point, x [L]
xii. density difference, ρ_a - ρ_e, $\Delta\rho$ [ML^{-3}]
xiii. gravity celerity, g [LT^{-2}]
xiv. viscocity, υ_a [L^2T^{-1}]
xv. hydraulics radius, R [L]
xvi. viscocity, υ_e [L^2T^{-1}]
xvii. density difference, ρ_a[ML^{-3}]

$$Q_a = \Phi\ (\Delta T, T_a, Q_e, d, x, y, z, \rho_a, \Delta\rho, u_a, u_e, \upsilon_a, \upsilon_e, g, R, B, A\ )$$

Number of parameters, m = 18

Number of main dimension, n = 3

$\therefore$ Number of group = m – n = 18 – 3

= 15

$Q_a = L^3\ T^{-1}$	$y = L$	$\rho_a = ML^{-3}$	$u_a = LT^{-1}$	$A = L^2$
$Q_e = L^3\ T^{-1}$	$d = L$	$\Delta\rho = ML^{-3}$	$\upsilon_a = L^2T^{-1}$	$B = L$
$\Delta T = 1$	$z = L$	$g = LT^{-2}$	$u_e = LT^{-1}$	
$T_e = 1$	$x = L$	$\upsilon_e = L^2T^{-1}$	$R = L$	

$$\pi_1 = \Phi\ (\pi_2, \pi_3, \pi_4, \pi_5, \pi_6, \pi_7, \pi_8, \pi_9, \pi_{10}, \pi_{11}, \pi_{12}, \pi_{13}, \pi_{14}, \pi_{15}, \pi_{16}, \pi_{17}, \pi_{18})$$

Number of repeated parameters = 3 [M, L, T]

Choose d, $\Delta\rho$ and u_a

Equation for every π:

$\pi_1 = \Delta T$

$\pi_2 = T_e$

$\pi_3 = d^{x3}\ \Delta\rho^{\ y3}\ u_a^{\ z3}\ x$

$\pi_8 = d^{x8}\ \Delta\rho^{\ y8}\ u_a^{\ z8}\ Q_e$

$\pi_9 = d^{x9}\ \Delta\rho^{\ y9}\ u_a^{\ z9}\ g$

$\pi_{10} = d^{x10}\ \Delta\rho^{\ y10}\ u_a^{\ z10}\ \upsilon_a$

$\pi_4 = d^{x4}\ \Delta\rho^{\ y4}\ u_a^{z4}\ y$

$\pi_5 = d^{x5}\ \Delta\rho^{\ y5}\ u_a^{z5}\ z$

$\pi_6 = d^{x6}\ \Delta\rho^{\ y6}\ u_a^{z6}\ \rho_a$

$\pi_7 = d^{x7}\ \Delta\rho^{\ y7}\ u_a^{z7}\ Q_a$

$\pi_{11} = d^{x11}\ \Delta\rho^{\ y11}\ u_a^{z11}\ u_e$

$\pi_{12} = d^{x12}\ \Delta\rho^{\ y12}\ u_a^{z12}\ R$

$\pi_{13} = d^{x13}\ \Delta\rho^{\ y13}\ u_a^{z13}\ \upsilon_e$

$\pi_{14} = d^{x14}\Delta\rho^{\ y14}\ u_a^{z14}\ A$

$\pi_{15} = d^{x15}\ \Delta\rho^{\ y15}\ u_a^{z15}\ B$

x, y and z for every π:

$\pi_1 = \Delta T$

$\pi_2 = T_e$

$\pi_3 = d^{x3}\ \Delta\rho^{\ y3}\ u_a^{z3}\ x$

$= [\ L\ ]^{\ x3}\ [\ ML^{-3}\ ]^{\ y3}\ [L\ T^{-1}\ ]^{\ z3}\ [\ L\ ]$

M, $\quad 0 = y^3$

T, $\quad 0 = -\ z^3,\ z^3 = 0$

L, $\quad 0 = x^3 - 3y^3 + z^3 + 1,\ x^3 = -1$

$\therefore\ \pi_3 = d^{-1}\ \Delta\rho^{\ 0}\ u_a^{\ 0}\ x$

$= \frac{x}{d}$

$\pi_4 = d^{x4}\ \Delta\rho^{\ y4}\ u_a^{\ z4}\ y$

$= [\ L\ ]^{\ x4}\ [\ ML^{-3}\ ]^{\ y4}\ [L\ T^{-1}\ ]^{\ z4}\ [\ L\ ]$

M, $\quad 0 = y^4$

T, $\quad 0 = -\ z^4,\ z^4 = 0$

L, $\quad 0 = x^4 - 3y^4 + z^4 + 1,\ x^4 = -1$

$\therefore\ \pi_4 = d^{-1}\ \Delta\rho^{\ 0}\ u_a^{\ 0}\ y$

$= \frac{y}{d}$

$\pi_5 = d^{x5}\ \Delta\rho^{\ y5}\ u_a^{\ z5}\ z$

$= [\ L\ ]^{\ x5}\ [\ ML^{-3}\ ]^{\ y5}\ [LT^{-1}\ ]^{\ z5}\ [\ L\ ]$

M, $\quad 0 = y^5$

T, $\quad 0 = -\ z^5,\ z^5 = 0$

L, $\quad 0 = x^5 - 3y^5 + z^5 + 1,\ x^5 = -1$

$\therefore\ \pi_6 = d^{-1}\ \Delta\rho^{\ 0}\ u_a^{\ 0}\ z$

$= \frac{z}{d}$

$\pi_6 = d^{x6}\ \Delta\rho^{\ y6}\ u_a^{\ z6}\ \rho_a$

$= [\ L\ ]^{\ x6}\ [\ ML^{-3}\ ]^{\ y6}\ [LT^{-1}\ ]^{\ z6}\ [ML^{-3}]$

M, $\quad 0 = y^6 + 1,\ y^6 = -1$

T, $\quad 0 = -\ z^6,\ z^6 = 0$

L, $\quad 0 = x^6 - 3y^6 + z^6 - 3,\ x^6 = 0$

$\therefore\ \pi_6 = d^0\ \Delta\rho^{\ -1}\ u_a^{\ 0}\ \rho_a$

$$= \frac{\rho_a}{\Delta\rho}$$

$\pi_7 = d^{x7}\ \Delta\rho^{\ y7}\ u_a^{\ z7}\ Q_a$

$= [\ L\ ]^{x7}\ [\ ML^{-3}\ ]^{y7}\ [LT^{-1}\ ]^{z7}\ [\ L^3T^{-1}\ ]$

M, $0 = y^7$

T, $0 = -\ z^7 - 1,\ z^7 = -1$

L, $0 = x^7 - 3y^7 + z^7 + 3,\ x^7 = -2$

$\therefore\ \pi_7 = d^{-2}\ \Delta\rho^{\ 0}\ u_a^{-1}\ Q_a$

$$= \frac{Q_a}{u_a d^2}$$

$\pi_8 = d^{x8}\ \Delta\rho^{\ y8}\ u_a^{\ z8}\ Q_e$

$= [\ L\ ]^{x8}\ [\ ML^{-3}\ ]^{y8}\ [LT^{-1}\ ]^{z8}\ [\ L^3T^{-1}\ ]$

M, $0 = y^8$

T, $0 = -\ z^8 - 1,\ z^8 = -1$

L, $0 = x^8 - 3y^8 + z^8 + 3,\ x^8 = -2$

$\therefore\ \pi_8 = d^{-2}\ \Delta\rho^{\ 0}\ u_a^{-1}\ Q_e$

$$= \frac{Q_e}{u_a d^2}$$

$\pi_9 = d^{x9}\ \Delta\rho^{\ y9}\ u_a^{\ z9}\ g$

$= [\ L\ ]^{x9}\ [\ ML^{-3}\ ]^{y9}\ [LT^{-1}\ ]^{z9}\ [LT^{-2}]$

M, $0 = y^9$

T, $0 = -\ z^9 - 2,\ z^9 = -2$

L, $0 = x^9 - 3y^9 + z^9 + 1,\ x^9 = 1$

$\therefore \pi_9 = d^1 \Delta\rho^{\,0} u_a^{-2} g$

$= \frac{gd}{u_a^{\,2}}$

$\pi_{10} = d^{x10} \Delta\rho^{\,y10} u_a^{\,z10} \upsilon_a$

$= [\,L\,]^{x10} [\,ML^{-3}\,]^{y10} [LT^{-1}\,]^{z10} [L^2T^{-1}]$

M, $0 = y^{10}$

T, $0 = -z^{10} - 1,\ z^{10} = -1$

L, $0 = x^{10} - 3y^{10} + z^{10} + 2,\ x^{10} = -1$

$\therefore \pi_{10} = d^{-1} \Delta\rho^{\,0} u_a^{-1} \upsilon_a$

$= \frac{\upsilon_a}{u_a d}$

$\pi_{11} = d^{x11} \Delta\rho^{\,y11} u_a^{\,z11} u_e$

$= [\,L\,]^{x11} [\,ML^{-3}\,]^{y11} [LT^{-1}\,]^{z11} [LT^{-1}]$

M, $0 = y^{11}$

T, $0 = -z^{11} - 1,\ z^{11} = -1$

L, $0 = x^{11} - 3y^{11} + z^{11} + 1,\ x^{11} = 0$

$\therefore \pi_{11} = d^0 \Delta\rho^{\,0} u_a^{-1} u_e$

$= \frac{u_e}{u_a}$

$\pi_{12} = d^{x12} \Delta\rho^{\,y12} u_a^{\,z12} R$

$= [\ L\ ]^{x12}\ [\ ML^{-3}\ ]^{y12}\ [L\ T^{-1}\ ]^{z12}\ [\ L\ ]$

M, $0 = y^{12}$

T, $0 = -\ z^{12},\ z^{12} = 0$

L, $0 = x^{12} - 3y^{12} + z^{12} + 1,\ x^{12} = -1$

$\therefore\ \pi_{12} = d^{-1}\ \Delta\rho^{\ 0}\ u_a^{\ 0}\ R$

$= \dfrac{R}{d}$

$\pi_{13} = d^{x13}\ \Delta\rho^{\ y13}\ u_a^{\ z13}\ \upsilon_e$

$= [\ L\ ]^{x13}\ [\ ML^{-3}\ ]^{y13}\ [LT^{-1}\ ]^{z13}\ [L^2T^{-1}]$

M, $0 = y^{13}$

T, $0 = -\ z^{13} - 1,\ z^{13} = -1$

L, $0 = x^{13} - 3y^{13} + z^{13} + 2,\ x^{13} = -1$

$\therefore\ \pi_{13} = d^{-1}\ \Delta\rho^{\ 0}\ u_a^{-1}\ \upsilon_e$

$= \dfrac{\upsilon_e}{u_a d}$

$\pi_{14} = d^{x14} \Delta\rho^{\ y14}\ u_a^{\ z14}\ A$

$= [\ L\ ]^{x14}\ [\ ML^{-3}\ ]^{y14}\ [L\ T^{-1}\ ]^{z14}\ [\ L^2\ ]$

M, $0 = y^{14}$

T, $0 = -\ z^{14},\ z^{14} = 0$

L, $0 = x^{14} - 3y^{14} + z^{14} + 2,\ x^{14} = -2$

$\therefore\ \pi_{14} = d^{-2}\ \Delta\rho^{\ 0}\ u_a^{\ 0}\ A$

$= \dfrac{A}{d^2}$

$\pi_{15} = d^{x15}\, \Delta\rho^{\,y15}\, u_a^{\,z15}\, B$

$= [\,L\,]^{x15}\, [\,ML^{-3}\,]^{y15}\, [L\,T^{-1}\,]^{z15}\, [\,L\,]$

M, $\quad 0 = y^{15}$

T, $\quad 0 = -\,z^{15},\ z^{15} = 0$

L, $\quad 0 = x^{15} - 3y^{15} + z^{15} + 1,\ x^{15} = -1$

$\therefore\ \pi_{15} = d^{-1}\, \Delta\rho^{\,0}\, u_a^{\,0}\, B$

$= \dfrac{B}{d}$

$$\frac{\Delta T}{T_e} = \Phi\left[\frac{x}{d}, \frac{y}{d}, \frac{z}{d}, \frac{\rho_a}{\Delta\rho}, \frac{Q_e}{u_a d^2}, \frac{g}{u_a^{\,2} d}, \frac{Q_a}{u_a d^2}, \frac{\upsilon_a}{u_a d}, \frac{\upsilon_e}{u_a d}, \frac{u_e}{u_a}, \frac{R}{d}, \frac{A}{d^2}, \frac{B}{d}\right]$$

$$\frac{\Delta T}{T_e} = \Phi\left[\frac{x}{d}, \frac{y}{d}, \frac{z}{d}, \frac{Q_a}{Q_e}, \frac{u_a R}{\upsilon_a}, \frac{u_e d}{\upsilon_e}, \frac{Ua}{\left(\dfrac{\Delta\rho}{\rho a} gH\right)^{\frac{1}{2}}}\right]$$

APPENDIX B (Data)

Qe = 0.133 liter/s

		Q10		Q20	
Station z/H	x/d	Excess Temperature, ΔT/Te	Dispersion Rate, K_T	Excess Temperature, ΔT/Te	Dispersion Rate, K_T
0.2	0	0.023	20.86	0.021	21.90
	30	0.010	48.80	0.006	76.00
	70	0.012	40.36	0.008	57.00
	110	0.019	25.22	0.002	228.00
	150	0.002	244.00	0.002	228.00
0.4	0	0.022	21.34	0.000	0.00
	30	0.006	77.67	0.004	110.00
	70	0.006	77.67	0.006	73.33
	110	0.023	19.92	0.006	73.33
	150	0.008	58.68	0.009	52.30
0.8	0	0.000	0.00	0.000	0.00
	30	0.004	108.50	0.004	123.00
	70	0.002	217.00	0.002	246.00
	110	0.030	14.68	0.002	246.00
	150	0.008	53.44	0.008	62.20

Qe = 0.05 liter/s

		Q10		Q20	
Station z/D	x/d	Excess Temperature, ΔT/Te	Dispersion Rate, K_T	Excess Temperature, ΔT/Te	Dispersion Rate, K_T
0.2	0	0.029	0.00	0.024	17.53
	30	0.010	43.99	0.002	198.65
	70	0.008	54.99	0.002	195.00
	110	0.021	20.90	0.017	24.71
	150	0.006	69.67	0.002	208.15
0.4	0	0.043	0.00	0.000	0.00
	30	0.014	33.83	0.011	38.51
	70	0.010	47.36	0.007	63.00
	110	0.019	24.19	0.006	73.26
	150	0.002	225.00	0.002	201.74
0.8	0	0.000	0.00	0.004	105.00
	30	0.006	66.65	0.012	36.47
	70	0.006	66.65	0.004	107.00
	110	0.013	31.67	0.016	27.12
	150	0.004	95.00	0.010	45.36

References

Adams, E.E. (1982). Dilution Analysis for Unidirectional Diffusers, *Journal of Hydraulic Division,* ASCE, Vol.108. No. HY3. 327-342.

Brennen, C.E. (2005). *Fundamentals of Multiphase Flow*. New York: Cambridge University Press.

Chow, V.T. (1959). *Open Channel Hydraulics*. Tokyo: McGraw-Hill. 7-14.

Davidson, M.J., Gaskin, S. and Wood, I.R. (2001). A Study of A Buoyant Axisymmetric Jet in a Small Co–Flow. *Journal of Hydraulic Research,* Vol. 40. No. 4. 477-489.

Fischer, H.B., List, E.J., Koh, R.C.Y., Imberger, J., Brooks, N.H. (1979). *Mixing in Inland and Coastal Waters*. San Diego, California: Academic Press. 105-145.

Jirka, G.H., Robert, L.D. and Steven, W.H. (1996). *User's Manual for CORMIX: A Hydrodynamic Mixing Zone Model and Decision Support System for Pollutant Discharge into Surface Waters.* United States of America: U.S. EPA. 152.

Kim, D.G. and Il, W.S. (1999). Modelling The Mixing of Heated Water Discharged From A Submerged Multiport Diffuser. *Journal of Hydraulic Research*. Vol. 38. 259-269.

Kuang, C.P and Lee, J.H.W. (2001). Effect of Downstream Control on Stability and Mixing of a Vertical Plane Jet in Confined Depth. *Journal of Hydraulic Research.* Vol. 39. No. 4. 375-391.

Lee, J.H.W. and Chu, V.H. (2003). *Turbulent Jets and Plumes-A Lagrangian Approach.* United States of America: Kluwer Academic Publishers. 211-247.

Martin, J.L. and McCutcheon, S.C. (1999). *Hydrodynamics and Transport for Water Quality Modeling.* Boca Raton: CRC Press, Inc. 91-92.

Mott, R.L. (1990) *Applied Fluid Mechanics, Third Edition*. University of Dayton,Ohio: Merrill Publishing Company.

Nuryazmeen Farhan Haron (2007). *Kajian Makmal Dan Permodelan Pelepasan Effluen Berhaba Dalam Saluran Terbuka.* Universiti Teknologi Malaysia. B.Eng (Civil) Thesis.

Perunding Utama Sdn. Bhd. (2003). *Detailed Environmental Impact Assessment For Proposed 3 X 700 MW Coal-Fired Power Plant at PTD 707 & 708, Tanjung Bin, Mukim Serkat, Daerah Pontian, Johor Darul Takzim.* Vol 2. Unpublished.

Ruzanna Ahmad Zahir (2005). *Kajian Makmal Pelepasan Haba Dalam Saluran Terbuka (Sistem Pelepasan Selari Dengan Aliran).* Universiti Teknologi Malaysia. . B.Eng (Civil) Thesis.

Rodi, W. (1982) *Turbulent Buoyant Jets and Plumes.* Great Britain: Pergamon Press Ltd.

Siti Asriza Sabri (2007). *Kajian Makmal Pelepasan Secara Serenjang Effluen Terma Pada Dasar Aliran Ambien Dalam Kawasan Medan Dekat*. Universiti Teknologi Malaysia. B.Eng (Civil) Thesis.

Stefan, H.G. and Hondzo, M. (1996). Heat Transport. in: Singh, V.P. and Hager, W.H. *Environmental Hydraulics*. Netherlands: Kluwer Academic Publishers. 189-218.

Zimmerman and Geldner (1978). Thermal loading of River Systems. In: Zoran, P.Z. *Thermal Effluent Disposal from Powe Generation. Washington:* Hemisphere Publishing Corporation. 175-194.

Zulkiflee Ibrahim (2006). *Notes on Hydraulics*. Vol 2. Universiti Teknologi Malaysia. Unpublished. 1-10.

Internet:

http://oceanlink.island.net/ask/pollution.html

http://rivrisk.tetratech.com/app_thermalrecirc.htm

http://www.aggreko.com/equipserv/Thermal-Discharge-Cooling.asp

http://www.pollutionissues.com/Te-Un/Thermal-Pollution.html

http://www.rpi.edu/dept/chem-eng/BiotechEnviron/Environmental